T.C.

TOKAT GAZİOSMANPAŞA UNIVERSITY

GRADUATE EDUCATION INSTITUDE

DEPARTMENT OF ELECTRICAL- ELECTRONIC ENGINEERING

MASTER PROGRAM

MAXIMUM POWER POINT TRACKER DESIGN FOR PHOTOVOLTAIC PANEL WITH ARTIFICIAL NEURAL NETWORK REFERENCED PID CONTROL METHOD

MASTER'S THESIS

Zedan Saeed Murad MURAD

Supervisor: Asst. Prof. Dr. Mehmet Serhat CAN

TOKAT-2023

THESIS STATEMENT

THESIS STATEMENT

I declare that the master's thesis on "Maximum Power Point Tracker Design For Photovoltaic Panel With Artificial Neural Network Referenced PID Control Method", which I prepared under the supervision of Asst. Prof. Dr. Mehmet Serhat CAN, according to the thesis writing guide of Tokat Gaziosmanpaşa University Graduate Education Institute, is an original study in accordance with scientific ethical values and rules, and that I will accept all kinds of legal sanctions if the opposite is determined.

28/07/2023
Thesis author Zedan Saeed Murad MURAD

ÖZET

Yüksek Lisans Tezi

Tokat Gaziosmanpaşa Üniversitesi

Fen Bilimleri Enstitüsü Eektrik-Elektronik Mühendisliği Anabilim Dalı

Zedan Saeed Murad MURAD

Danışman: Asst. Prof. Dr. Mehmet Serhat Can

Yıl: 2023, Sayfa: 57

Bu tezde, fotovoltaik (PV) güç sistemleri için Yapay Sinir Ağı (YSA) çıkışını referans değer olarak kullanan Oransal Integral Türevsel (PID) denetleyici esaslı bir Maksimum Güç Noktası İzleme (MPPT) yöntemi önerilmektedir. Önerilen yöntem geleneksel MPPT yöntemleri olan Değiştir Gözle (P&O) ve Artan İletkenlik (IC) MPPT algoritmaları için uyarlanmıştır. Önerilen yöntemde YSA anlık güneş ışınımı ve PV panel sıcaklığına bakarak olması gereken maksimum güç noktasını (MPP) belirlemekte ve böylece değişken güneş ışınımına ve panel sıcaklığına göre adaptif bir referans değer elde edilmektedir. Daha sonra bu referans MPP değer ile PV anlık gücü arasındaki fark alınmak suretiyle bir hata değeri oluşturulmaktadır. Son olarak bu hata değeri bir PID denetleyiciden geçirilerek bir kontrol işareti elde edilmektedir. Bu kontrol işareti ise PO ve IC algoritmalarındaki normalde sabit olarak alınan çevrim oranı yerine kullanılmaktadır. Böylece değişken güneş ışınımına ve panel sıcaklığına göre adaptif ve bir referans değere göre çevrim oranı üretilmektedir. Bu ise P&O ve IC yöntemlerinde karşılaşılan dezavantajları giderebilmektedir. Çalışma, yükselten tipi bir DC-DC çevirici ve bir evirici üzerinden şebekeye bağlı 100 kW gücündeki bir PV dizisi üzerinde benzetim çalışmaları ile test edilmiştir. Testlerde gerçek ortam koşullarını temsil edebilmek için farklı ışınım ve PV panel sıcaklık koşulları dikkate alınmıştır. Bulgulara göre önerilen yöntemin, geleneksel P&O ve IC yöntemlerine göre daha az güç dalgalanmasına, yüksek hızlı yanıta ve çevrim oranında daha az dalgacık oranına sahip olduğu gözlemlenmiştir.

Anahtar Kelimeler: Maksimum Güç Noktası İzleme, MPPT, Fotovoltaik Güç Sistemi, PV, Yapay Sinir Ağı.

ABSTRACT

Master of Science

University of Tokat Gaziosmanpaşa

Graduate School of Natural and Applied Sciences

Department of Electrical Electronic Engineering

Zedan Saeed Murad MURAD

Supervisor: Asst. Prof. Dr. Mehmet Serhat Can

Year: 2023, Page: 57

In this thesis, a Proportional Integral Derivative (PID) controller based Maximum Power Point Tracking (MPPT) method is proposed for photovoltaic (PV) power systems, which uses the Artificial Neural Network (ANN) output as a reference value. The proposed method is adapted for the traditional MPPT methods, change by perturb and observe (P&O) and Incremental Conductance (IC) MPPT algorithms. In the proposed method, ANN determines the required maximum power point (MPP) by looking at the instantaneous solar radiation and PV panel temperature, and thus an adaptive reference value is obtained according to the variable solar radiation and panel temperature. An error value is then generated by taking the difference between this reference MPP value and the PV instantaneous power. Finally, this error value is passed through a PID controller to obtain a control signal. This control signal is used instead of the normally fixed duty ratio in P&O and IC algorithms. Thus, adaptive duty ratio is produced according to variable solar radiation and panel temperature and according to a reference value. This can eliminate the disadvantages encountered in P&O and IC methods. The study has been tested by simulation studies on a 100 kW PV array connected to the grid via a boost type DC-DC converter and an inverter. Different radiation and PV panel temperature conditions were taken into account in order to represent the real ambient conditions in the tests. According to the findings, it has been observed that the proposed method has less power fluctuation, high speed response and less ripple ratio in duty ratio compared to traditional P&O and IC methods.

Keywords: Maximum Power Point Tracking, MPPT, photovoltaic power system, PV, artificial neural network.

ACKNOWLEDGMENT

First and foremost, praises and thanks to the God, the Almighty, for His showers of blessings throughout my research work to complete the research successfully.

I would like to express my deep and sincere gratitude to Asst. Prof. Dr. Mehmet Serhat Can, my project supervisor, for providing me with excellent advice and courage from the beginning to the end of my MSc. project work. It was a great privilege and honor to work and study under his guidance. I am extremely grateful for what he has offered me. I would also like to thank him for his friendship, empathy, and great sense of humor.

My great appreciation goes to my family specially my father and mother who have supported me all these years. Their love and motivation provide me the spirit to finish this thesis successfully.

I would also like to thank all of the academic staff at the University of Tokat Gaziosmanpaşa University, Electrical-Electronic Engineering department, especially, Prof. Dr. Ulaş EMİNOĞLU and to Asst. Prof. Dr. Tufan DUĞRUER. And my special thanks to my wife that was always beside me and never stopped giving the motivation.

Finally, my thanks go to all of my friends who have supported me to complete the research work directly or indirectly.

Zedan Saeed Murad MURAD

TABLE OF CONTENT

LIST OF SYMBOLS AND ABBRIVATIONS

I_{ph}	PV cell's photocurrent (A)
I_{sc}	PV cells short-circuit current (A)
I_{pv}	PV cell's output current (A)
I_o	PV cell's saturation current (A)
I_{rs}	Reverse saturation current (A)
V_{oc}	Open circuit voltage (V)
V_{pv}	PV cells Output voltage (V)
$V_{d\text{-}min}$	Converter input voltage (V)
R_s	PV cell internal series resistance (Ω)
R_p	PV cell internal parallel resistance (Ω)
R_{sh}	PV cell Shunt resistance (Ω)
ANN	Artificial Neural Network
IC	Incremental Conductance
P&O	Perturb and Observe
PID	proportional Integral Derivative
N_s	Number of cells connected in series
N_p	Number of cells connected in parallel
η	Efficiency
D	Duty cycle
f_s	Switching frequency (Hz)
FF	Fill factor
G	PV Irradiance (W/m^2)
T	PV temperature (^oC)
T_{rk}	Reference temperature at 298 K
T_{ak}	Ambient temperature (^oC)
A	Ideality factor = 1.6
q	Electron charge = 1.6×10^{-19} C
E_g	Band gap for silicon = 1.1 eV
K	Boltzmann constant = 1.3805×10^{-23} J/K

LIST OF FIGURE

1. INTRODUCTION

Renewable energy technologies and structures are gaining popularity due to their quiet and clean nature. Renewable energy technologies exist in a wide range of forms. Due to the nature and natural behavior of renewable energy, it can generate either DC or AC electricity. The present scenario encourages us to connect additional renewable energy sources to the networks. PV systems are one of the most rapidly increasing and widely utilized power sources in modern electric technologies. Despite the fact that solar panel structures typically have high production costs and low energy transformation efficiency (Kumaresh et al., 2014). The most important factor for replacing traditional energy sources with environmentally friendly natural sources is determining how to capture the greatest amount of energy and deliver the greatest amount of power at the lowest cost for the specified load in the electrical network (M. A. Sasi, 2017).

One of the best renewable energy sources is solar energy. It is a significant advantage because solar energy systems don't release dangerous chemicals into the environment. Furthermore, the fact that it may be used practically anywhere is a significant advantage. It is now employed in a wide range of applications and sizes, including vehicles, houses, farms, residential area etc. Mechanical generators and engines are not utilized in the production of electricity from solar energy, as they are in the generation of electricity from other renewable resources. This is a significant benefit with regard to both maintenance and costs. In addition to all of the benefits, the efficiency of converting solar energy to electricity is in the range of 15-20%. Environmental parameters such as radiation and ambient temperature are also major factors influencing the output power of solar energy systems (Luo, L, et al,. 2020).

Solar energy has the ability to be a limitless source of energy in the years to come. Solar energy is energy in the form of photons produced by the Sun that is received and turned into thermal or electrical energy. The photoelectric effect is used to generate electricity using solar energy. The photoelectric effect occurs when the energy contained in photons dispersed from the sun causes free electrons to be released on a surface. Solar energy is converted into electricity using photovoltaic (PV) panels constructed of semiconductor materials silicon and selenium. Depending on the application, buck, boost, or buck-boost DC-DC converters should be utilized to decrease or increase the voltage from the PV (Dinçer, F. 2011).

PV output power is affected by solar radiation and temperature. Seasonal fluctuations, changes in the angle of reflections of sunlight based on the path of the sun through the day, and shading caused by variables like clouding and dusting are all factors that impact the radiation and temperature of the PV. The electricity generated by PV varies depending on this component. The maximum power point (MPP) is the power value generated by the PV for each radiation and temperature condition. Maximum Power Point Tracking (MPPT) is the practice of maintaining the PV's output power at the MPP point (Rajesh and Mabel. 2015). In research, many approaches

for MPPT have been proposed. Constant Voltage (CV), Open-Circuit Voltage (OCV), Short-Circuit Current (SCC), Perturb and Observer (P&O), incremental conductance (INC), Extreme Seeking Control (ESC), Ripple Correlation Control (RCC), Fuzzy Logic Control (FLC), Artificial Neural Network (ANN), and Proportional-Integral-Derivative (PID) based approaches are examples of these.

The CV algorithm is a simplified MPPT control approach. This approach aims to determine the voltage of the solar panel module at the MPP (V_{ref} or V_{mpp}) and maintain the solar panel module's instantaneous operating voltage at the established V_{ref} value. Temperature and radiation are not considered. It is expected that by obtaining the V_{ref} value, the MPP at the panel output is retrieved approximately (Karami, N, et al., 2017). Under specific radiation and temperature situations, V_{ref} is obtained. Because of the fluctuation of radiation and temperature, it cannot precisely monitor the MPP (Ko, J. S, et al., 2020).

Another basic MPPT approach is OCV. It is a more developed type of CV approach. As with the CV approach, no fixed reference voltage is used. A fixed reference voltage is not utilized as in the CV approach. At the running period, the load is deactivated, and the current open circuit voltage is measured again for the current irradiance and temperature values. The V_{ref} value is derived by computing the formula $V_{mpp} = V_{oc} \times k_1\ 0.7 < k_1 \leq 0.8$ for each determined open-circuit voltage. Then the CV method is operated. This approach is simplified, however the frequent disconnection and resuming of the load generate discontinuities and losses in the supplying of the load. In this way, too, the actual MPP is hard to capture. The SCC approach is an approach that performs comparable operations to the OCV technique over a flow of data. Disconnecting the load from time to time has a detrimental impact on efficiency in this manner as well. In this approach, the short-circuit current in the MPP is computed using the following equation: $I_{mpp} = I_{sc} \times k_2 0.78 \leq k_2 \leq 0.92$ (Ko, J. S, et al., 2020).

When the panels in a photovoltaic system receive varying radiation, the traditional P&O approach has certain issues. It has a long tracking period and large steady-state vibrations in these instances (Karami, N, et al., 2017). For duty modification, the traditional P&O approach has a set iteration step size. Increasing the step size speeds up tracking while causing steady-state vibrations around the MPP. When the step is shortened, the steady-state vibrations are dampened, but the tracking speed is reduced by one. P&O approaches with variable iteration step sizes have been proposed in the literature to address this issue. The distance to the MPP is considered in these procedures. When the output power is close to MPP, larger steps are chosen for faster tracking, whereas smaller steps are preferable for reduced oscillation. (Yüksek and Mete, 2022) introduced a P&O-based variable step size approach to MPPT. Another popular MPPT approach is the Incremental Conductance (IC) method. The electrical conductivity of the photovoltaic panel is compared with the rise in conductivity in this approach (Kayisli, 2023). The Incremental Conductance (IC) approach is utilized to overcome the disadvantage of the P&O approach under rapidly changing atmospheric circumstances (Christopher and Ramesh, 2013). The dP/dV ratio is used to make a conclusion in this case. At the MPP point on the power-

voltage graph, *dP/dV* equals zero. The formula *I/V = dI/dV* is obtained from here. In this formula, *I/V* represents the PV conductance, and *dI/dV* represents the incremental conductance. The position of the present operating point on the power-voltage graph is determined by evaluating these two ratios.

The Artificial Neural Network technique is an excellent strategy to generate mathematical mapping via learning between the variables of the input and output. of nonlinear systems (Ahmed, Emad M, et al., 2022). Although artificial neural networks are trained with a limited number of inputs, they generate outcomes by generalizing to a large number of uninformed inputs. This feature is commonly employed in a variety of MPPT investigations. Some MPPT studies (Chun-hua, et al., 2009) made use of a fuzzy neural network (FNN). ANN has been employed in some research to estimate the optimal current and voltage values in the MPP (Dzung, et al, 2010), and in others to foresee the MPP voltage. In this study, the ANN calculates the global MPP voltage based on the instantaneous radiation and temperature value, the FLC provides the control signal to achieve the MPP based on this voltage value.

In this thesis, a Maximum Power Point Tracking (MPPT) method based on Artificial Neural Network (ANN) and PID controller is proposed. In the study, ANN was trained using instantaneous solar radiation and PV panel temperature values. Thus, ANN finds the actual MPP value that should be according to each new solar radiation and PV panel temperature value. An error value is calculated by taking the difference between this real MPP value, which the ANN finds for each new situation, and the instantaneous PV panel output power. This error value is used as the input error value for the PID controller. The control signal generated by PID is used instead of the normally fixed conversion rate in traditional P&O and IC algorithms. Thus, adaptive conversion rate is produced according to variable solar radiation and panel temperature and according to a reference value. This can eliminate the disadvantages encountered in P&O and IC methods. A 100 kW PV array output was connected to an electric grid via a boost DC-DC converter and an inverter, and simulation studies were carried out for different solar radiation and PV panel temperature values.

2. LITERATURE REVIEW

Many academics have studied various strategies for tracking the Maximum Power Point (MPP) of PV arrays. This chapter analyzes all of the material gathered from significant research on PV system DC-DC converter applications and develops an MPPT controller for a stand-alone and grid-connected PV system. Journals, conferences, research papers and books are the primary sources of this knowledge.

Litrán, S. P.et al., (2009) presents a method for regulating the MPPT of a PV system. A solar array, a load coupled to a DC/AC inverter, and a DC/DC converter comprise the system. The recommended solution, which is based on Sliding Mode Control, enables direct control of the power converter. The efficiency of the proposed approach is demonstrated in this study through some realistic simulation results, and the system's adaptability and dependability are also investigated.

Shih and Lu, (2010) developed a Fuzzy Neural Network (FNN) control system with a boost DC/DC converter for the solar cells MPPT controller. The FNN system, which blends fuzzy theory with neural networks, has two advantages: predictability neural network learning and data processing. First, a suitable framework was developed. By changing the learning settings and the weight of connections in the neuron network it can track the maximum power point of the solar PV cell. Finally, when compared to alternative qualitative controllers, the proposed MPPT approach exhibited the quickest tracking speed and the highest efficiency.

Gothandaraman, V, et al., (2011). Presents enhanced modeling of Solar Photovoltaic (SPV) arrays The GA approach is used to extract the greatest power from the SPV source. The ideal power and concomitant values of voltage, temperature, and irradiance levels for various insolation levels were employed to train the ANN. Then, for any environmental changes, a GA-based offline learning ANN is utilized to provide the reference voltage comparable to the peak power. The proposed method has been evaluated in a variety of scenarios, with error percentages ranging from 0.05% to 4.46%. This mistake can be decreased by increasing the quantity of data available for ANN training.

Ouali and Salah (2011) introduced and investigated two innovative MPPT algorithms, the first based on the FLC and the second on the ANN. FLC and ANN that change over time can be used to simulate nonlinear dynamical complex systems. The recommended FLC and ANN methods entail commanding a DC-DC boost inverter to instantaneously compute the MPPT from meteorological information such as PV cell temperature and sun insolation. Additionally, these two MPPT give a simplified solution at a low cost of deployment. Based on the results, the MPPT controller used FLC to provide more power than the ANN controller.

According to Badamchizadeh, et al. (2012), this paper demonstrates how a NN is utilized to track the greatest point of power. The error backpropagation technique is used to train a neural

network. The benefits of employing a neural network include It can precisely and rapidly track the MPP. In this technique, a neural network is used to determine the maximum power point reference voltage under varied atmospheric conditions. The MPP may be tracked by appropriately regulating the DC-DC boost converter, and simulation results were obtained using Matlab/Simulink to validate theory analysis.

Pikutis, et al. (2012) investigated the use of artificial neural networks in solar panel MPPT. It has been emphasized the usage of an online learning ANN to enhance the MPPT technique for PV panels. After creating a mathematical model of the system, the MPPT is implemented using the Matlab/Simulink framework and the IC method and the radial basis function ANN. The estimation of system performance was based on a variety of criteria; all of these studies indicated that ANN may improve overall system efficiency by 10%. ANN also minimizes variance in power output (*P*) while enhancing MPPT responsiveness and robustness. With trained ANN, MPPT efficiency may be improved by up to 99%.

Silvestre, et al. (2012) established a new way for examining the key components of a grid-connected PV system using modeling and simulation in this research. The results of the simulations, which were based on an evaluation of the major PV module features, showed that the PV module's supplied model properly represents the *I-V* characteristic. The full system simulation, which contains the PV generator, single-phase phase inverter, and inverter modeling, is an excellent alternative for analyzing the energy production of the entire plant that is connected to the utility grid.

Jamasb, et al. (2013), Several MPPT methods were investigated in this article, and their benefits and disadvantages were compared using simulations. These strategies have been classified into three categories: hybrid, online, and offline. Several MPPT methods are compared in terms of the PV system's dynamic responsiveness, attainable efficiency, and implementation variables using simulations on the Matlab/Simulink platform. As implementation factors, the relative ease of implementation, costs, and hardware requirements were investigated. Under nearly equal structures, hybrid approaches outperform. The findings reveal that design choices impact both system performance and dynamic responsiveness.

Albarbar, et al. (2014) created a smart grid-connected solar power model using temperature and irradiance as inputs and power as output under various situations. Matlab/Simulink software was used to implement the model. Based on MPPT implementation, an ANN approach is applied to maximize the produced power. The suggested model's dynamic behavior is investigated under various operating situations. The suggested model and its control method provide an appropriate instrument for optimizing smart grid performance.

Shahid and Singh (2016) proposed ANN and FLC approaches for single ended primary inductor converters in this research report. There has been a wide variety of irradiation levels used. Explored, such as continuous, slow, and fast shifting, which contributes to the uniqueness of

their work. Maximum power tracking techniques were evaluated for accuracy based on the time it takes to trace the MPP and other important characteristics such as stability, efficiency, fluctuations, settling time, and voltage and power overshoot before reaching MPP. This experiment shows that when using ANN, the system's reaction is superior to FLC because it is faster and more accurate in monitoring MPP, but it has higher voltage and duty cycle overshooting when the irradiation level varies. The ANN technology is 99.86% efficient and delivers 98.93 KW of power energy to the grid, whereas the FLC technology is 95.48% efficient and delivers 94.47 KW of power electricity to the system.

In order to improve the efficiency of PV panels, El-khattam, et al. (2018) propose a FLC-based MPPT algorithm. Under partial shading conditions (PSC), the authors want to give the maximum amount of energy to the load. As a consequence, it has been discovered that the suggested technique fast achieves global MPP under PSC and has little output power fluctuation stand-alone PV systems are those that employ PV panels to satisfy the end user's power demands without being linked to an external network.

Rahman and Islam (2019) suggested a hybrid strategy that used ANN and P&O techniques. Photovoltaic (PV) current and voltage readings are utilized as input data for ANN and P&O. Depending on the scenario, a controller picks the output of an ANN or P&O and applies it to the input of a PI controller. The appropriate control signal is generated using PI.

Gündoğdu and Çelikel (2020) suggest an MPPT method based on an Artificial Neural Network (ANN) to maximize the efficiency of PV panels. The suggested PSC approach is compared to the INC and P&O algorithms. In MPP tracking, it is discovered that the ANN-based MPPT approach is better the other two techniques. Furthermore, among the algorithms used, the ANN-based MPPT algorithms are shown to be the most efficient.

According to Leow, et al., (2020), photovoltaic panels are strongly impacted by changes in solar irradiance and temperatures, resulting in the generation of unstable energy that can't be provided directly to the batteries or the load. As a result, the author proposes that a DC-DC boost converter founded on the PID controller unit be utilized for controlling the work cycle. A 12-volt battery is charged using a boost converter. The findings of the boost transformer simulation revealed that the transformer regulates the current and voltage moving to charge the battery, as well as protecting the battery from harm and extending its life.

Abdelwahab, et al. (2020) introduced the Maximum Power Point Tracking MPPT technologies, which depends on the modified perturbation and observation (MP&O) approach and is designed to be utilized in solar energy systems to harvest the greatest energy from them under various irradiance and temperatures conditions. The photovoltaic system was simulated in the MATLAB/Simulink environment with an entire circuit design of the MP&O-based charge controller, and the simulation results were compared to the results of traditional methods (P&0, IC). Whereas outcomes rapidly demonstrated the superiority of the old MP&O algorithm under

various irradiance and temperatures conditions, the suggested technique gives excellent performance and improves the system's efficiency from 94% to 98%.

Meng, X et al., (2020) examined the MPP current and voltage estimation performance of classical ANN and Bayesian-ANN systems. They also looked at the MPPT performances. (Farhat, et al., 2013) computed MPP in the Multilayer Perceptron (MLP) model using PV radiation and temperature measurements.

A hybrid approach for the P&O approach was presented in (Jiang, et al., 2021). ANN takes radiation and temperature measurements as input data and calculates the voltage value (V_{mpp}) at the MPP point as output in this approach. The ANN output is then used as an input by the PI controller. Whereas PI generates the reference voltage (V_{ref}) for the classic P&O approach.

Nasser, et al. (2021) develop and simulate a simple, low-cost MPP tracker. The suggested technique is based on disrupting PV power to get the best MPP in different temperature and irradiance condition. The relationship between the PV panel's perceived input resistance, load resistance, and duty cycle is obtained by mathematically evaluating the fly back converter. The equivalent input resistance was modified as a result of the duty adjustment, and the MPP was obtained. Changes in PV power cause the duty cycle to be changed. PSIM software is used to build and simulate the proposed approach, and the MPP tracker is produced instantly using basic C-block code. In the end, within fast changes in environmental conditions, the proposed tracker is successful in collecting the MPP with minor ripple resolution.

Mohamed, et al. (2021) provided that in order to enhance the efficiency of the photovoltaic system and improve the generating capacity of the system, which is dependent on the amount of solar irradiation and temperatures, the authors used conventional approaches in MPPT technology, in which they utilized two approaches, the P&O and the IC, in addition to the utilize of approaches based on artificial intelligence, such as the MPPT approaches based on the unit FLC. The three approaches were simulated in Matlab/Simulink and the outcomes have been compared to figure out which approaches are optimal for improving efficiency under changing environmental conditions.

Rodriguez, et al. (2021) demonstrated the desire for solar energy has expanded, particularly in the past few years, due to the simplicity of collecting it, and it is an energy that does not run out and is accessible on most days of the year, but its difficulty is its level of efficiency. Is the most significant impediment, and it has become the main objective of most academics' efforts to identify ways to improve the efficiency of solar systems. In order to get the most energy out of the solar panels. This approach utilizes a number of algorithms. The study also focused at the ANN approach, in which the speed and accuracy of MPP tracking are affected by the kind of the algorithm utilized in the hidden layer and the quality of its learning. According to the study, the use of ANN-based MPPT technology results in average efficiency of up to 98% in identical conditions, high convergence velocity, and decreased oscillations around the MPP.

Roy, et al., (2021) attempted to identify VMPP by feeding radiation and temperature into an ANN. The difference between the ANN output and the PV instantaneous voltage was then calculated and used to calculate the error value. The control signal for MPPT is obtained by feeding this error value into a PID controller.

Ali, et. (2021) presented and evaluated a hybrid technique that included Metaheuristic, Fuzzy-Logic, and ANN methodologies on a Grid-Connected Photovoltaic system. Another research evaluated the MPP estimation performances of ANN and FLC algorithms. The Genetic Algorithm (GA), Particle Swarm Optimization (PSO), and Imperial Competitive Algorithm (ICA) techniques are used to optimize ANN weights (Fathi and Parian, 2021).

Meng, X, et al., (2021) discovered a preliminary MPP value using ANN. They presented an adaptive P&O approach for partial and complete cloud scenarios. Instead of ANN, a similar investigation was conducted utilizing the Adaptive Neuro-Fuzzy Inference System (Ahmed, et al., 2022).

3. MATERIAL AND METHOD

3.1 Material

3.1.1 PV cell and PV array

PV cells may directly generate electrical energy from sunlight. Under the photovoltaic effect (Patel, 2006). PV cells are constructed from two semiconductor layers, positive layer and negative layer Sunlight energy is derived from photons, which are little particles Figure (3.1). Photons travel through and are absorbed by the solar cell when a photovoltaic cell is exposed to sunlight. In the closed circuit, the produced electrons create electrical current, which has an electrical voltage on the load. Typically, one cell's current is (28-35 mA) and its voltage is approximately (0.5-0.6 V). (Onar and Khaligh ,2019).

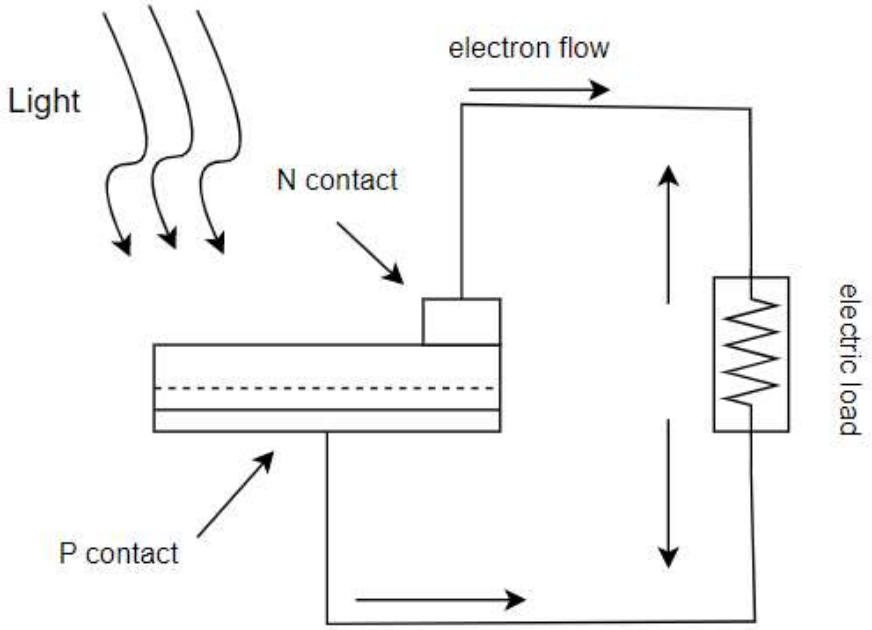

Figure 3.1. The work principle of photovoltaic cell.

To generate the required voltage and power, cells are connected in series and parallel. (Hoffmann and Goetzberger, 2005). Increase the number of series cells connected to increase the output voltage Figure (3.2 (b)). When solar cells are connected, each cell receives the same current. The sum of the voltages from each cell makes up the total voltage, and the overall output voltage can be determined as follows:

$$V_{out} = V_1 + V_2 + V_3 \dots \dots V_n \quad (3.1)$$

The equation can be rewritten as follows because the voltages of the cells are equal:

$$V_{out} = V * N_s \quad (3.2)$$

Where:

Ns is series connected cells in array.

V is a PV voltage

Increase the parallel-connected cell's output current to increase power output Figure (3.2 (a)). Since the voltage between every cell is the same, the complete current equivalents the amount of all cell flows, and the total output current is determined as follows:

$$I_{out} = I_1 + I_2 + I_3 \dots \dots I_n. \quad (3.3)$$

Since the cells

$$I_{out} = I * N_P \quad (3.4)$$

Where:

N_p is parallel connected cells in array.

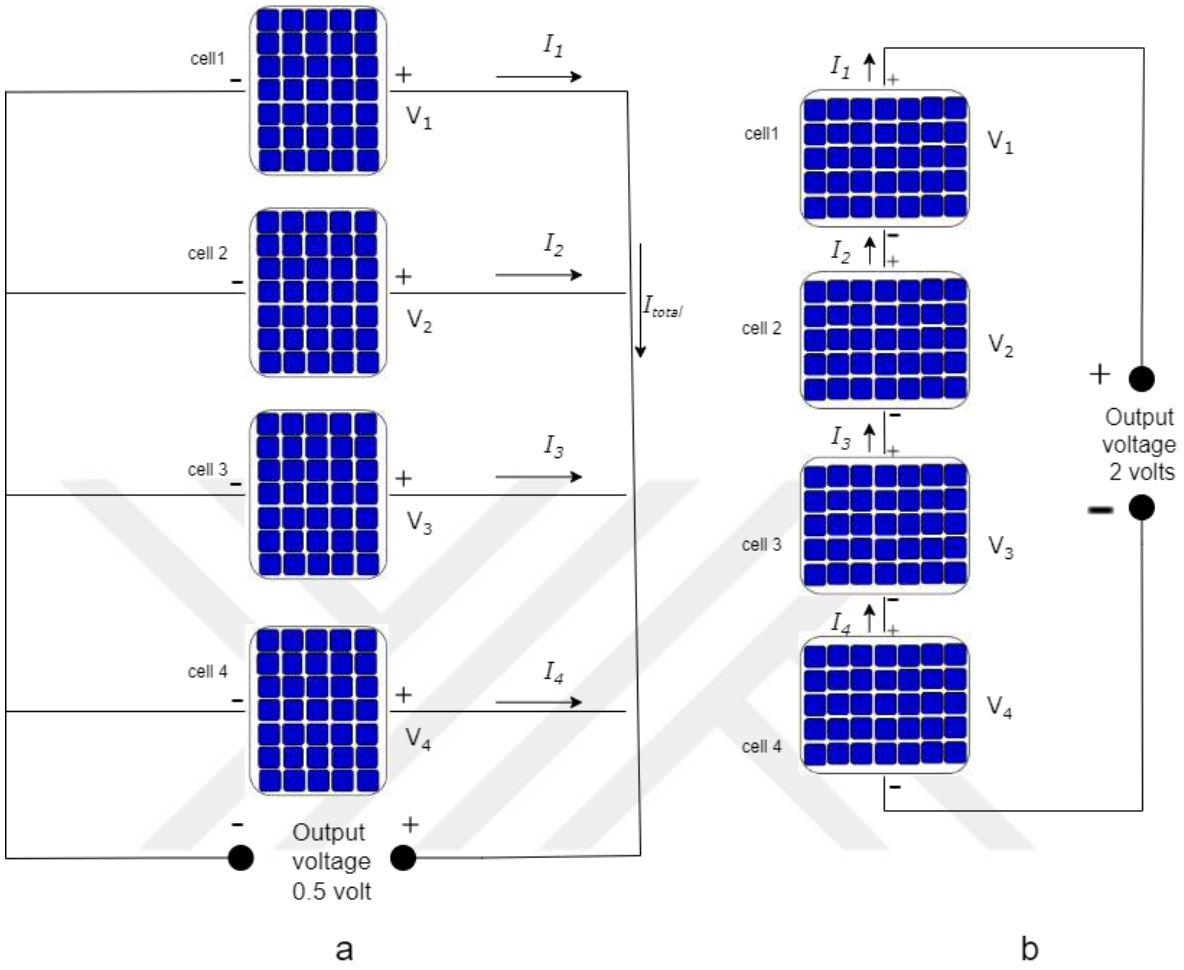

Figure 3.2. Solar cell connection. (a) Cell connected in parallel. (b) Cell connected in series.

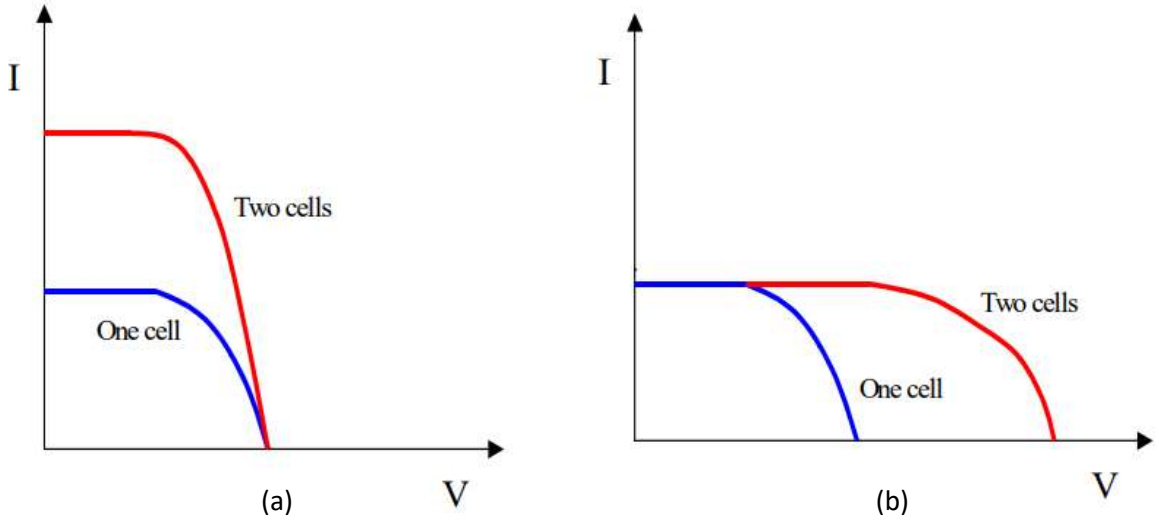

Figure 3.3: The impact of cell addition on I-V curves. (a) paralel cell. (b) series cell. (Bindner, et al. 2001).

PV solar cells can be classified into three forms: solar cells, which are single photovoltaic (PV) cells that convert light into energy in a single unit. Module photovoltaic (PV) is a board with a number of parallel and series-connected solar cells. PV system connections of PV modules in series and parallel are known as a PV array.

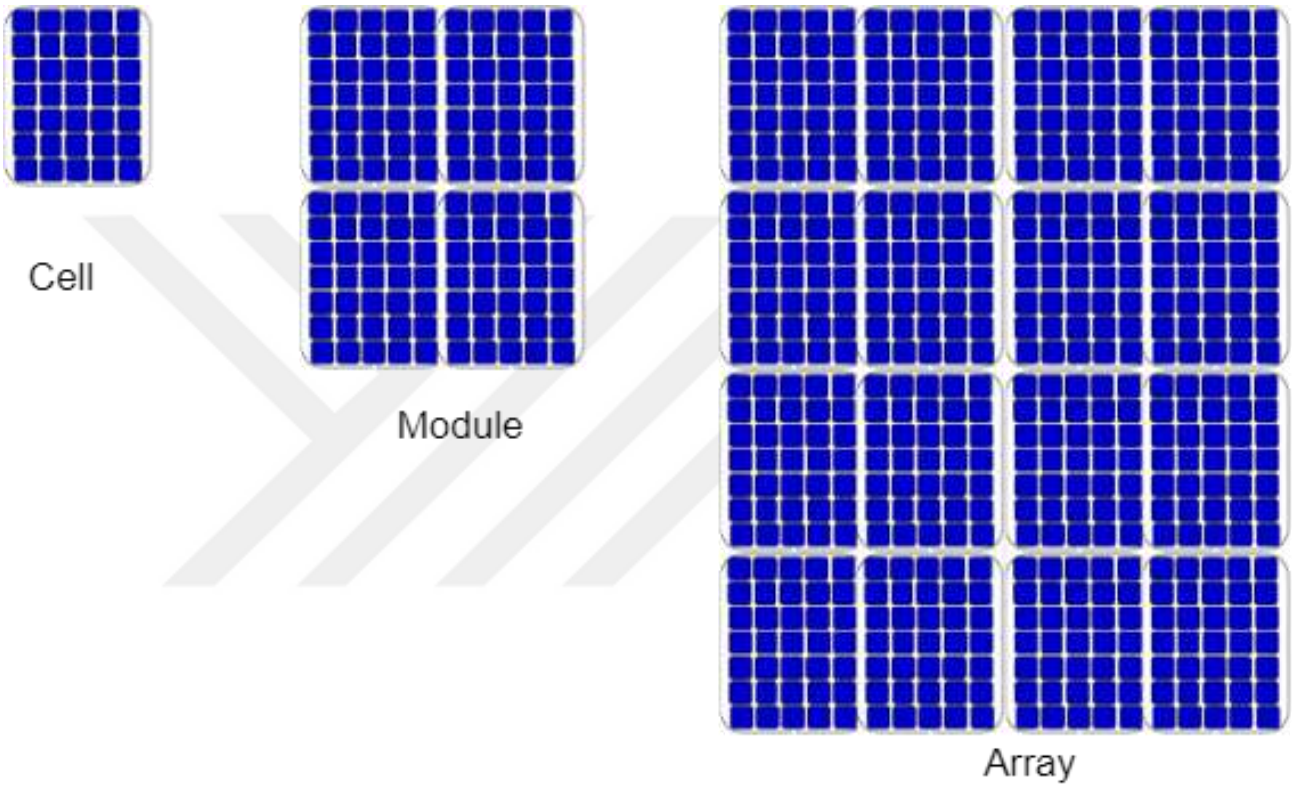

Figure 3.4. Different form of the PV units.

3.1.1.1 PV cell equivalent circuit

The analogous circuits of PV cells can be thought of as p-n semiconductor junctions. Direct current (DC) is produced by the terminal when the cell is exposed to sunlight. Solar irradiation, temperature, and load current all have an effect on produced current (Ibrahim, et al., 2013). Figure (3.5) illustrates the cell's equivalent electrical circuit. Furthermore, the following equations represent the output current characteristic:

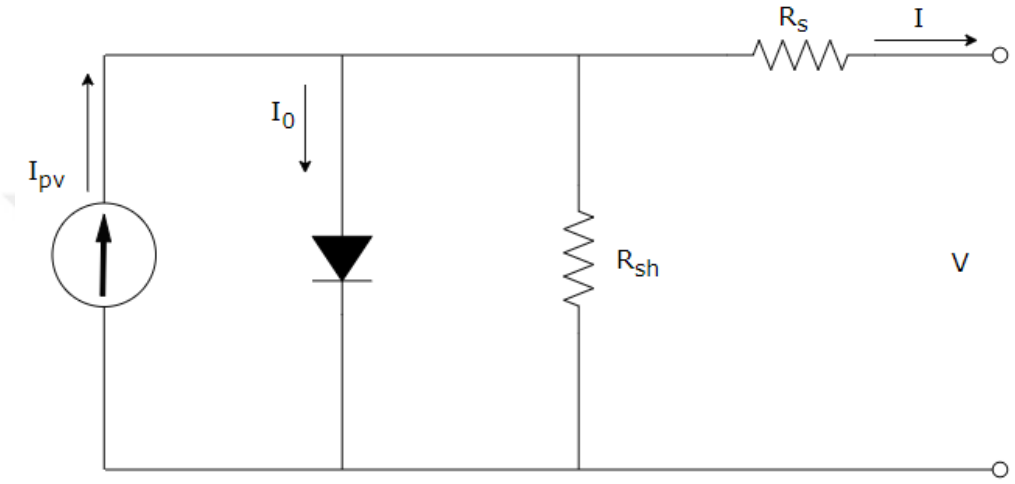

Figure 3.5. A single PV cell's electrical equivalent circuit.

$$I_{pv} = I_{ph} - I_0 * \left[e^{\left(\frac{V_{pv}+I_{pv}*R_s}{A*K*T_{ak}}\right)} - 1 \right] - \left(\frac{V_{pv} + I_{pv} * R_s}{R_{sh}}\right) \tag{3.5}$$

$$I_{ph} = I_{sc} + K_1 * (T_{ak} - T_{rk}) * G \tag{3.6}$$

$$I_0 = I_{rs} * \left(\frac{T_{ak}}{T_{rk}}\right)^3 * e^{\left[\left(\frac{q*E_g}{A*K}\right)*\left(\frac{1}{T_{ak}}-\frac{1}{T_{rk}}\right)\right]} \tag{3.7}$$

$$I_{rs} = \frac{I_{scr}}{\left[e^{\left(\frac{q(V_{oc}+I_{pv}*R_s}{A*K*T_{ak}}\right)} - 1 \right]} \tag{3.8}$$

The current equation becomes as follows for large arrays of series and parallel connected cells:

$$I = I_{ph} * N_P - I_0 * N_P * \left(e^{\left(\frac{q(V_{pv}+I_{pv}*R_s}{N_s*A*K*T_{ak^*}}-1\right)} - \frac{V_{pv}\frac{N_s}{N_p} + I_{pv} * R_s}{R_p} \right) \tag{3.9}$$

3.1.1.2 Characteristic of the PV cell output

The ratio between current and voltage is expressed as a curve and is used to determine the properties of a PV cell. If the cell's terminal is connected to a variable resistance *R*, the Current-Voltage (*I-V*) characteristic determines the operating point in the load. Figure (3.6). The load characteristic can be represented using a straight line with a slope of 1/R. The amount of power delivered to the load is determined only by the resistance value. As a result, when the load at *R* is low, the cell runs as a constant current nearly equal to the cell's I_{sc} in the region of the curve between *M* and *N*. Moreover, when the load at *R* is high, the cell will run in the area of the curve between *P* and *S*, where it operates as a constant voltage source with a value close to V_{oc} (Bindner, et al., 2001).

The I-V and P-V curves of a PV cell have the shape illustrated in Figure (3.6), and power is generated for a given radiation intensity. (Fujita and pelc, 2002).

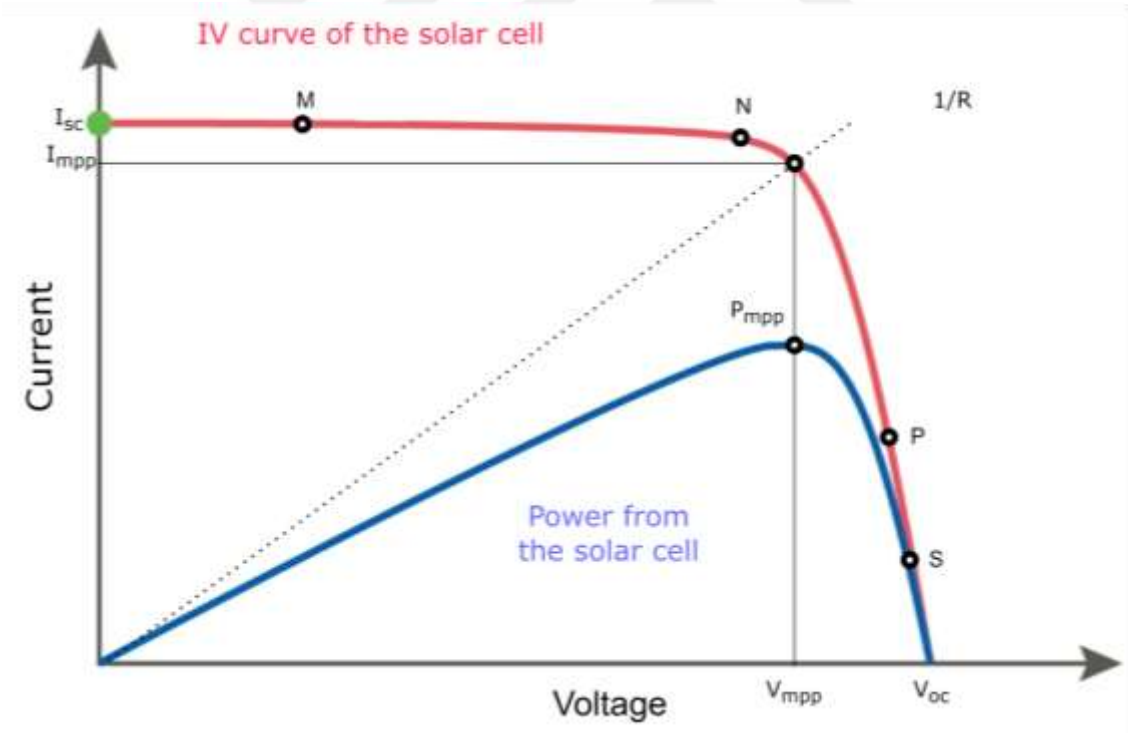

Figure 3.6. Power curves (I-V).

Real PV cells may be described by the fundamental characteristics indicated in the above figure (Bindner, et al., 2001).

Short-circuit current (I_{sc}). Is the current passing into the solar cell when the voltage in the solar cell is zero. Open circuit voltage (V_{oc}) the voltage that passes through the diode when no load is applied is proportional to the cell. Maximum power (P_{MPP}) maximum power received by the load when the cell is operating at point *P* (I_{MPP}, V_{MPP}) where the power dissipated by the load is maximum:

$$P_{MPP} = I_{MPP} * V_{MPP} \tag{3.10}$$

Maximum power operating current (IMPP) The current is generated when the cell reaches the MPP point on the *I-V* curve. Maximum power operating voltage (VMPP) The voltage is generated when the cell reaches the MPP point on the *I-V* curve.

3.1.1.3 Cell efficiency

A PV cell's efficiency conversion is a significant feature. The cell output power to radiation power received ratio is:

$$\eta = \frac{I_{MPP} * V_{MPP}}{G} = \frac{FF * I_{sc} * V_{oc}}{G} \tag{3.11}$$

Where Fill Factor (*FF*) is the product of I_{sc} and V_{oc} and the distributional ratio of MPP to load (Bindner, et al., 2001). Typically, its value is more than 0.7. The format of the *FF* is as follows:

$$FF = \frac{I_{MPP} * V_{MPP}}{V_{oc} * I_{sc}} \tag{3.12}$$

Cell's efficiency is determined under standard test conditions (STC) of T = 25 °C, G = 1000 kw/m^2.

3.1.1.4 Affection of Temperature and Irradiance on PV output

A PV solar cell's output power is determined by changes in operation *G* and *T*. Figure (3.7). The I_{sc} and V_{oc} of the solar cell rise as the amount of sunlight increases. From Equation (3.6) I_{ph} has an approximately linear relationship with *G*. When the temperature rises, the V_{oc} falls and the I_{sc} rises (Onar and Khaligh, 2009). Figure (3.7) depicts the effect of altering *G* and *T* on cell properties.

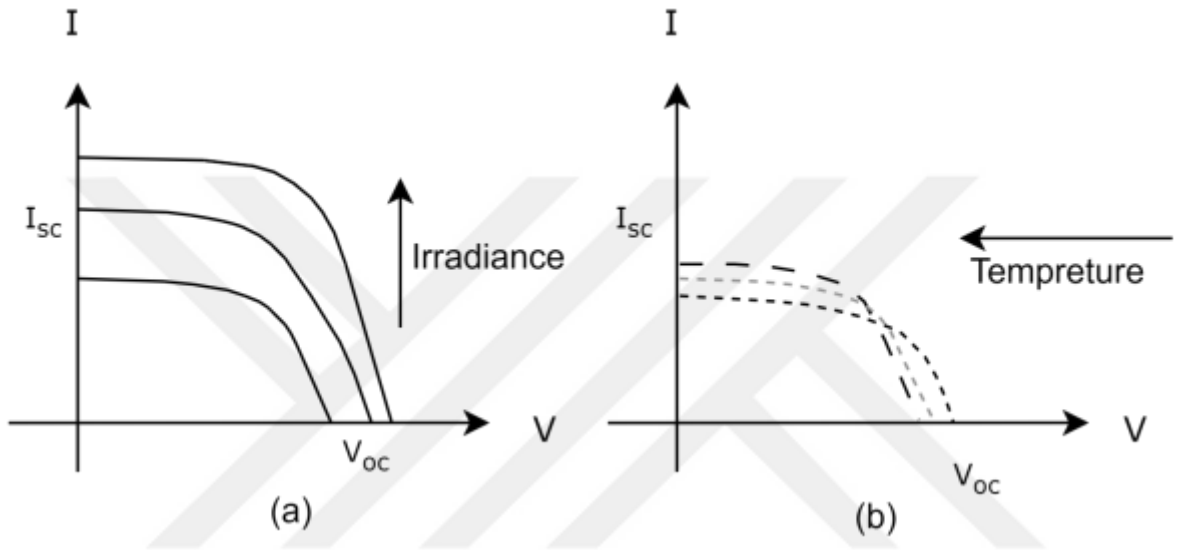

Figure 3.7. Radiation and temperature effects on cell I-V characteristics. a) Radiation effects. (b) Temperature effects. (Onar and Khaligh, 2009).

3.1.1.5 PV system's forms

One of the following forms is possible for a photovoltaic PV system:

Off-grid or stand-alone systems have no connection to the grid network and are typically utilized in remote areas. They have several uses such as house lighting, camping, washing machine and so on. The grid- connected system type does not require batteries to operate at night from the grid network because it is directly connected to the power grid. When there is no power available, the battery works as a backup supply in the hybrid system.

3.1.2 Boost DC-DC converter

Two applications for boost converter functioning are the regenerative braking circuit of DC motors and controlled DC power sources. With this type of converter, the output voltage is always larger than the input voltage. Since the output voltage of MPPT systems must be greater than the input voltage, the step-up converter can be used in those systems. For example, in a grid-connected system, the boost converter remains a high output voltage even when the PV array voltage falls to low levels.

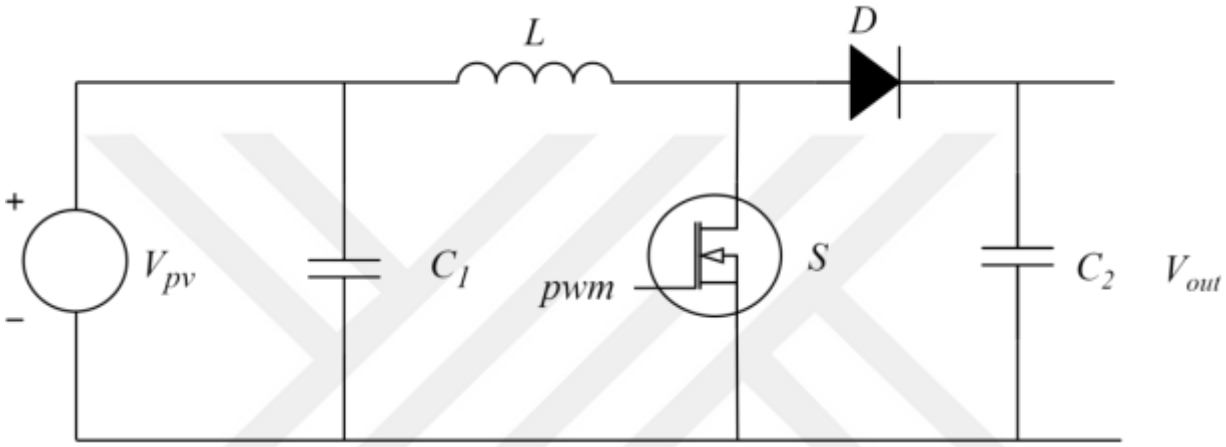

Figure 3.8 Boost DC-DC converter circuit.

The diode becomes opposite based when the switch (*S*) is energized. As a result of the linear increase in the inductor's current caused by the input voltage source, the output stage is separated and the capacitor is partially drained, providing the current load. When the switch is switched off during the second period, the diode conducts, and the output stage receives energy from the inductor and input source. In continuous conduction mode, when the inductor current flows constantly (Mohan and Undeland, 2007), the inductor current waveform is shown in Figure (3.9).

To provide the electricity generated by the PV array to the load, a two-stage power electronics system consisting of a step-up DC/DC converter and an inverter is utilized. To keep the load voltage constant, a DC-DC boost converter is employed between the PV array and the inverter. A DC-DC converter is an essential part of an MPPT system. They are often used in DC power supplies to transform uncontrolled DC inputs into controlled DC outputs at specified voltage and current rates. A three-phase sine wave six step inverter receives the voltage provided by the DC-DC converter, and a three-phase fixed amplitude and fixed frequency supply is produced to feed an inverter as input. When the converter is operating at steady-state, the duty cycle (*D*) can be calculated via Equation (3.13) (Mohan and Undeland, 2007).

$$D = 1 - \frac{V_{d-min}}{V_{out}}\eta \tag{3.13}$$

Where (D) represent the duty cycle ratio, (η) represent the efficiency, (V_d) represent the converter input voltage and (V_{out}) represent the converter output voltage. According to equation (3.13), increasing the duty cycle ratio (D) increases the value of the output voltage, V_{out}. Furthermore, changes in the duty cycle ratio affect the converter's input and output current.

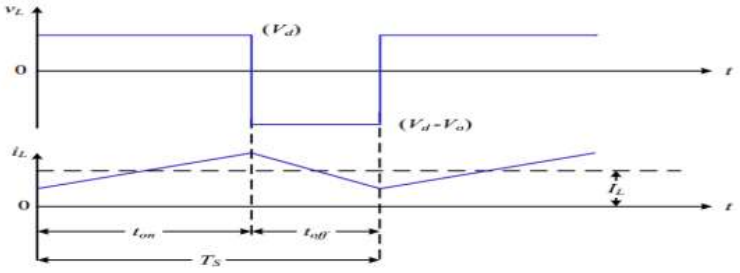

Figure.3.9 DC-DC boost converter inductor current and voltage waveforms in continuous current. (Mohan and Undeland, 2007).

The following equations may be used to determine the filter inductor and capacitor needed to run the converter in continuous conduction mode.

$$L = \frac{V_d}{\Delta I_L f_s} D \tag{3.14}$$

$$C = \frac{I_0}{\Delta V_0 f_s} \tag{3.15}$$

Where f_s represent the switching frequency, I_{in} represent the input current and I_o represent the output current, ΔV_o is the peak-to-peak ripple voltage at the output, ΔI_L change in inductor current.

3.1.3 Grid connected PV system

Grid connected PV system recently have become most used in industrial region. To find out, we must first discover an effective MPPT technique that produces more power when combined. The general framework of a grid-connected PV system is depicted in Figure (3.10). PV cells, which are also a source of electricity or a producer of light energy, are layered in series or parallel to optimize the benefit of solar radiation. Another component that is primarily regulated during MPPT control unit connection is the DC-DC converter. (Souba et al,. 2016). With this device, the switches function as a tracker to conserve energy to the fullest extent feasible under all operating situations. The three-phase DC-AC bridge inverter circuit is connected to the grid through a typical step-up transformer (Kassmi, et al., 2019).

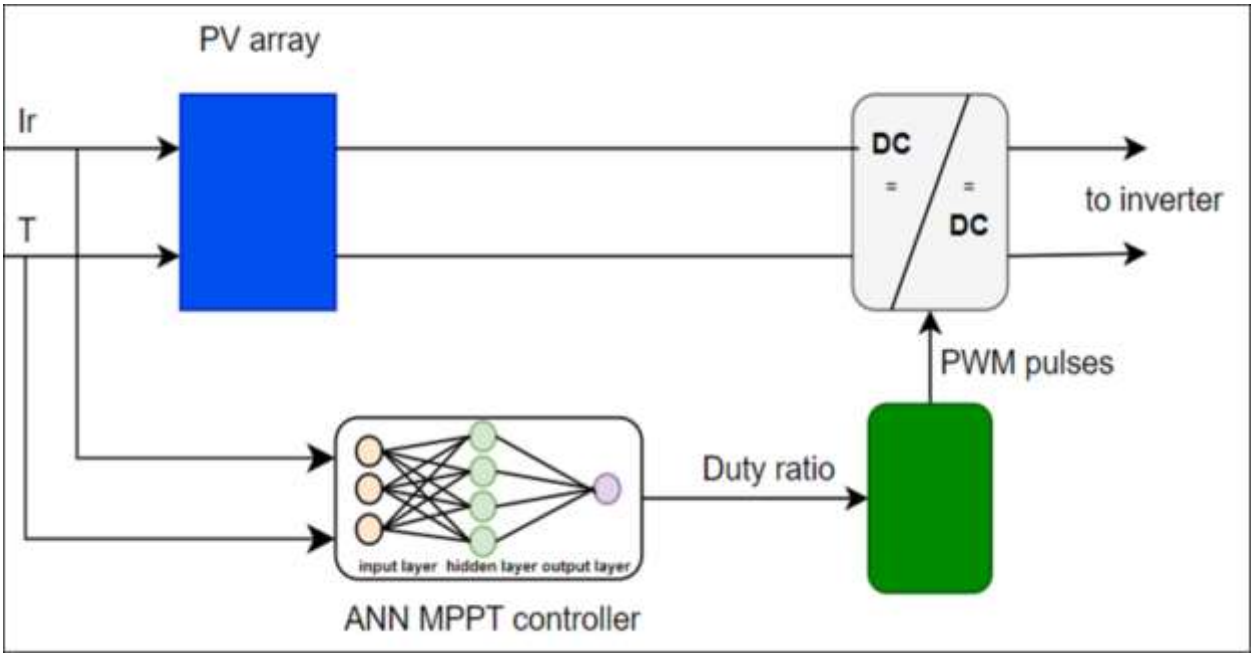

Figure 3.10. Block diagram of Grid-connected PV system.

PV panel modeling, DC-DC converter, and algorithm are the most important variables to consider while designing an MPPT controller.

3.2 Methods

3.2.1 Maximum Power Point Tracking (MPPT)

Solar energy is converted into electrical electricity. It is transformed dependent on the conversion's efficiency. When a solar module achieves the maximum power production, its conversion efficiency is high (Huang, 2011).

Nevertheless, the power point is influenced by temperature and solar insolation uncertainty. As illustrated in Figure (3.11), this results in a changing *I-V* curve.

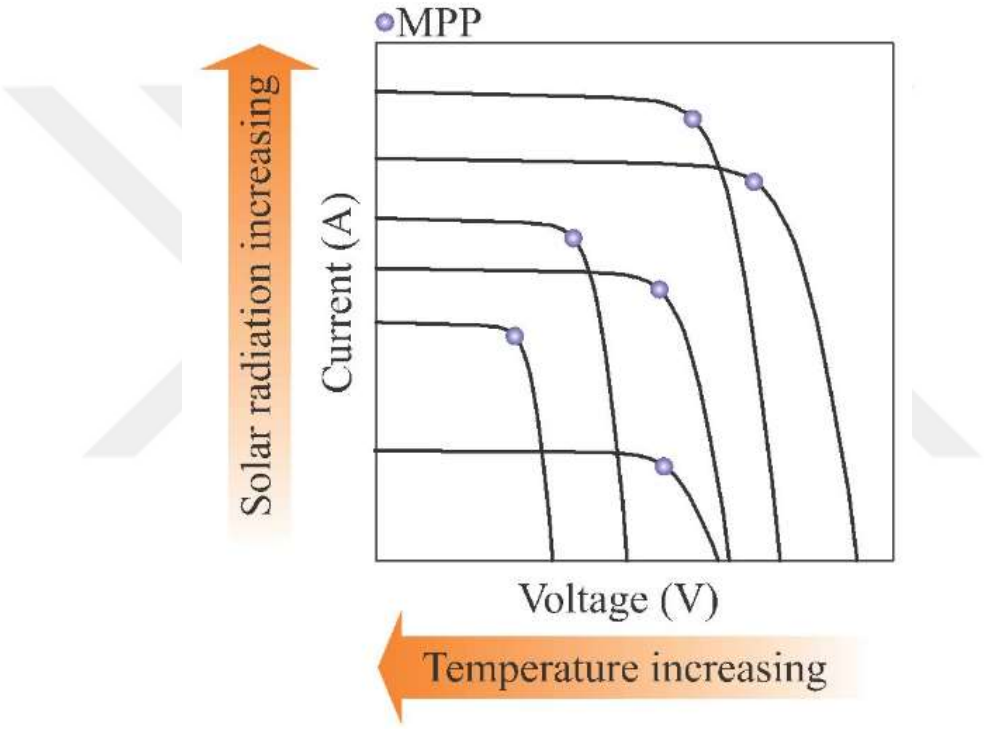

Figure 3.11. MPP over the I-V curves with varying insolation and temperature. (Martins and Coelho, 2012).

The MPP varies in response to differences in solar radiation and temperature. Consequence, Maximum Power Point Tracking methods are required to automatically establish the MPP as the operating point for a wide range of inputs temperature and irradiance (Saravana, et al., 2014).

An MPPT device, as seen in Figure (3.12), is essentially a DC-DC converter that connects solar modules to a load that is regulated by a tracking algorithm.

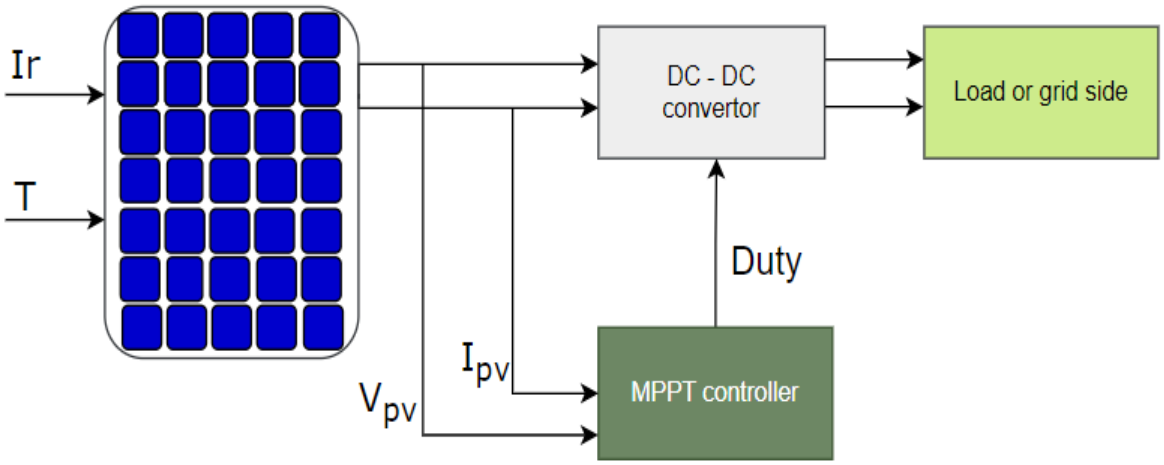

Figure 3.12. A DC-DC converter and tracking controller from an MPPT structure.

MPPT research is based on two important approaches: maximum power point tracking and power converter topology optimization. A power converter configuration is a way for identifying a suitable DC-DC converter for MPPT operation. The MPPT algorithm, on the other hand, is used to control the DC-DC converter (Zaki, et al., 2012).

Ultimately, a dynamic MPPT system is developed by combining an effective DC-DC converter with an acceptable tracking algorithm (Mathew and Vinay, 2014).

3.2.2 Tracking Algorithm

3.2.2.1 Perturb and Observe (P&O)

Perturb and Observe is the most common and easiest MPPT approach. While Hill Climbing used duty cycle as a control variable, P&O used the voltage of the PV panels. This is the major difference between P&O and Hill climbing. (Bohorquez, et al., (2010). Shujaee, et al., (2012). Chapman, and Esram (2007). Pradhan and Subudhi, (2012). In the original Perturb and Observe approach, there is a small but steady disturbance in the reference voltage of the PV module, then subtracted from the operating voltage and the determined error is passed through PI. A comparator compares the PI output to the carrier signal, therefore a pulse width modulation (PWM) signal is generated. Assume the PV panel's voltage is raised and the output power is calculated. The voltage rises in the same manner as the panel's output power. The direction is totally reversed if the output power falls. The purpose is to force the operating voltage towards V_{mpp}, the operational voltage varies between positive and negative increments, and the output voltage oscillates around V_{mpp}. (Lazaro, et al., (2006). Powers and Sullivan, (1993). Bhatanger and Nema,(2013) The P&O algorithm flowchart in Figure (3.13) clearly shows this loop.

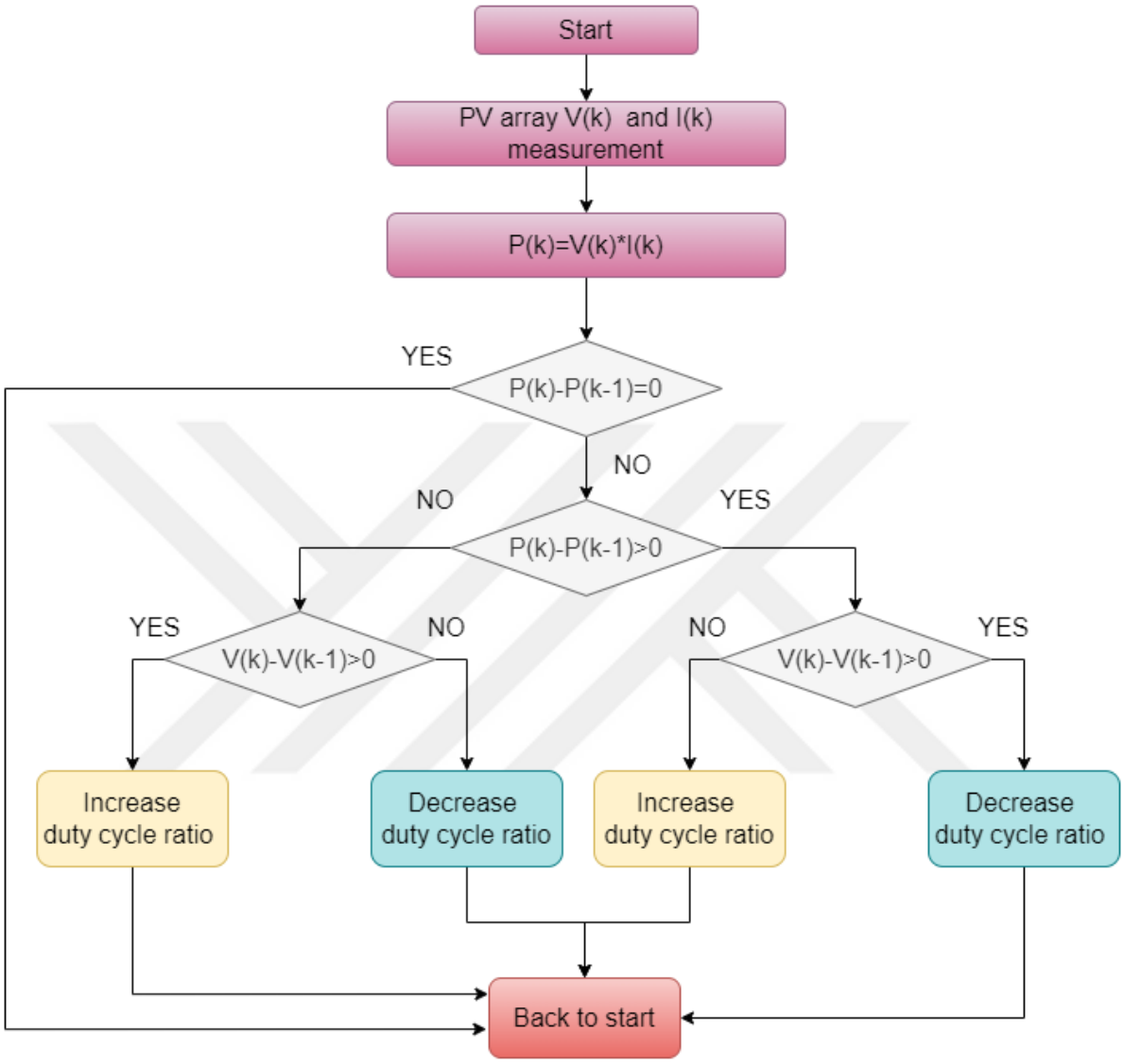

Figure 3.13. Perturb and Observe algorithm flowchart.

The P&O MPPT technique has a number of issues that significantly affect the PV system's output power. The perturbation size is one of them, limiting the speed of convergence and determining the amplitude of oscillations around the V_{mpp}. It cannot be positioned correctly on V_{mpp} (Veerachary, (2008). Lazaro, et al., (2006). Adaptive perturbation size strategies have been proposed as a solution to this problem in the literature. (Vitelli, et al., (2004). Massoud, et al., (2011).

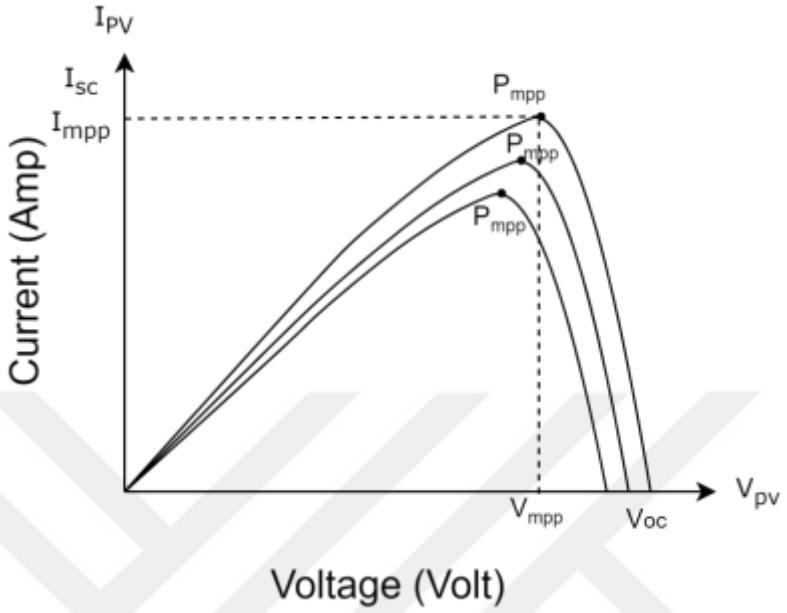

Figure 3.14. P&O algorithm unpredictable behavior under changeable atmospheric conditions. (Bohorquez, et al., 2010).

As can be seen in Figure (3.14), this method does not give the correct perturbation direction even when atmospheric conditions change rapidly, when the operational point varies from the V_{mpp} point. Nonetheless, simplicity, the absence of PV panel characteristics, and ease of installation might be characterized as positives (Bhatanger and Nema, (2013). Bohorquez, et al., (2010).

3.2.2.2 Incremental Conductance (IC)

Basically, the Incremental Conductance approach relies on the fact that the derivative of the power of the solar panel with voltages as seen in Equation (3.15). (Mekhilef and Safari, 2011).

$$\frac{dP}{dV} = 0$$

$$\frac{d(IV)}{dV} = I + V\frac{dI}{dV} \cong I + V\frac{\Delta I}{\Delta V} \tag{3.16}$$

The following is an explanation of Equation (3.16):

$$\frac{\Delta I}{\Delta V} = -\frac{1}{V}, \qquad at\ MPP$$

$$\frac{\Delta I}{\Delta V} > -\frac{1}{V}, left\ of\ MPP$$

$$\frac{\Delta I}{\Delta V} < -\frac{1}{V}, right\ of\ MPP$$

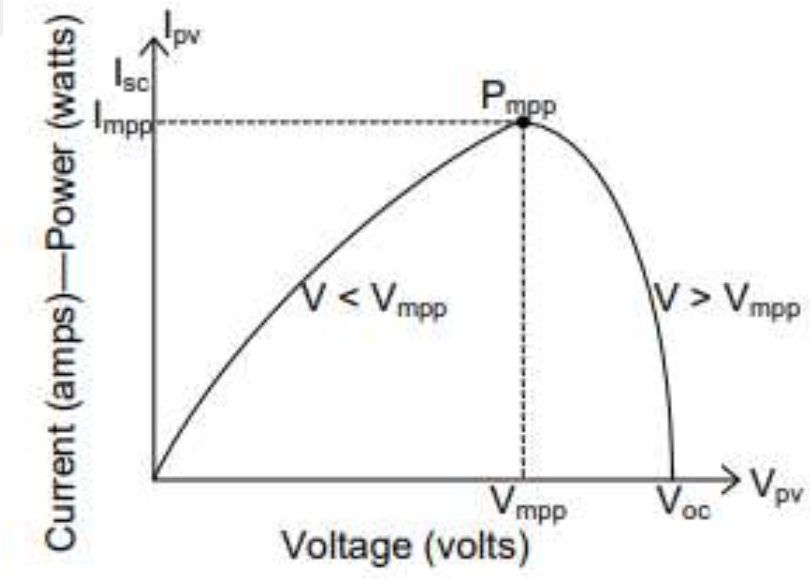

Figure 3.15. PV panel operating voltage state. (Mekhilef and Safari, 2011).

The Incremental Conductance approach reduces fluctuation in operating voltage around MPP, one of the P&O algorithm's most significant difficulties. As previously stated, when the operating voltage approaches the Maximum Power Point (MPP), when d = 0**,** the algorithm recognizes this and the voltage rise stops. (Bhatanger and Nema, 2013). Until the

atmospheric conditions change, the PV panel continues running as illustrated in Figure (3.15). (Chapman and Esram, (2007). Osakada, et al., (1995).

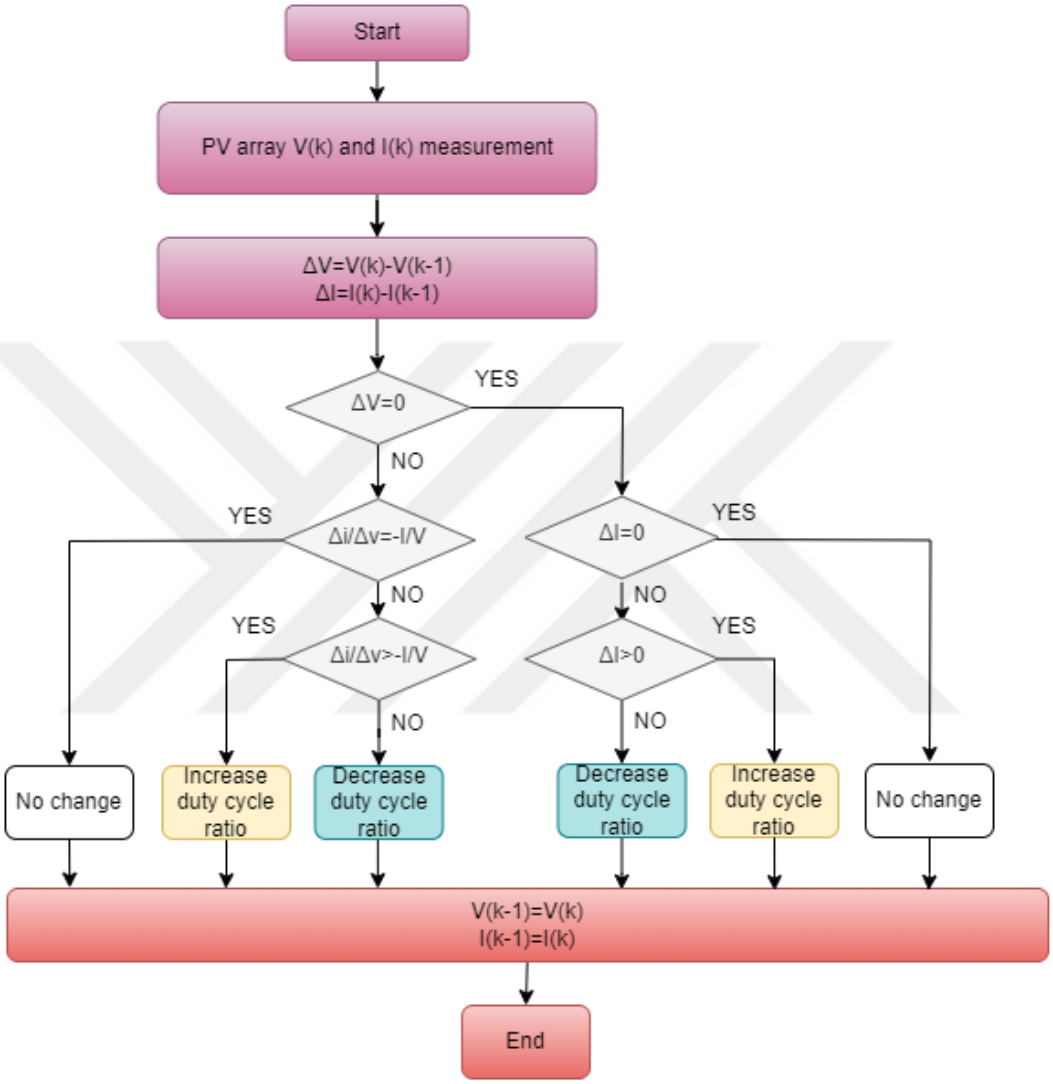

Figure 3.16. Incremental Conductance algorithm flowchart.

The rate of increment size is a significant problem in the Perturb and Observe approach. Since the convergence speed is mostly determined by this parameter (Osakada, et al., (1995). Zhao and Eltawil, (2013). The variable step-size INC approach is used to manage this scenario. Depending on where the operating voltage is, the step size varies. (Guerrero, et al., (2011). Bennett, et al., (2013). In terms of tracking speed, tracking accuracy, and efficiency, the INC approach outperforms the P&O method. Additionally, the INC technique produces more efficient results under partial shading conditions. The INC MPPT approach, on the other hand, is more sophisticated, and its performance in real applications is impacted by noise and errors in measured control values. (Mekhilef and Safari, 2011).

3.2.2.3 Artificial Neural Networks (ANNs)

Artificial Neural Networks are networks that comprising a massive parallel network of neurons that mimic the organic neural network of the human system. It can do a variety of tasks in a relatively short period of time, especially when compared to today's high-speed computers. The behavior of networks is commonly applied in modeling complicated interactions between linear and nonlinear systems' inputs and outputs, as well as in data mapping.

Three-layer network restriction can be as follows:

- Input layer: it consists nodes representing input characteristics. The hidden layer has connections to all other nodes. During the training process, the connections' weightiness will change.
- Hidden layer: After combining each input node's multiplication with connected weights, the activation function is used to calculate the hidden node's output. Typical functions include sigmoid, ramp, and threshold.
- Output layer: To obtain the output, the same procedure as in the hidden layer is applied. Figure (3.17) shows network three layers.

There are several network structures (Hagan, et al., 2014). Multi-layer feed forward networks are the neural network structure type utilized to develop MPPT controllers. In the input layer, the inputs to the MPPT controller are typically two-node PV provided parameters such as radiation and temperature, whereas the output layer is made up of single output nodes. As output resolution, the controller estimates the adapter operating duty cycle by analyzing these inputs. As the activation function for each node, the sigmoid function is commonly employed. Before being used in the system, ANN must be trained off-line. Figure (3.17) shows a three-layer network. In the neural network, the input layer (i) is comprised of two nodes that correspond to the input variables (x_1, x_2). The hidden layer (j) consists of three nodes, while the output layer (y) includes a singular neuron within the hidden layer, neurons connect to previous neurons. (Hagan, et al., 2014).

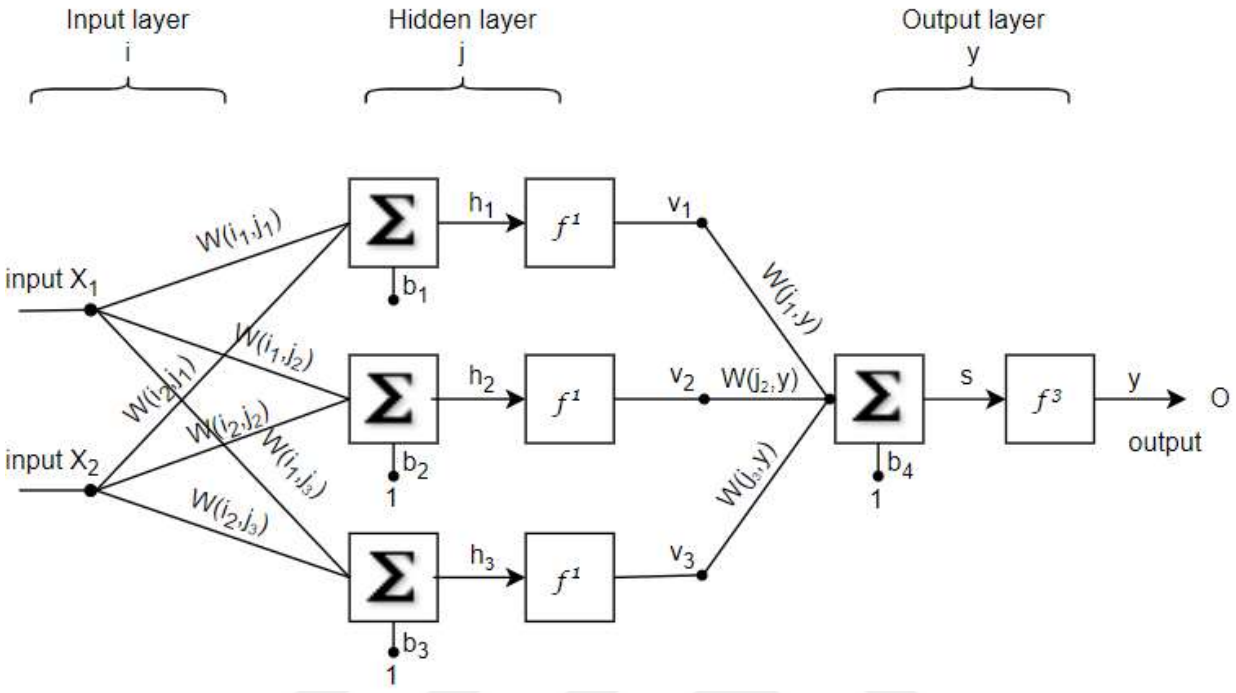

Figure 3.17. Feed forward network three layer of multi-layer. (Hagan, et al., 2014).

Output of the network may be estimated using the following formula:

First determine h_1, h_2 and h_3

$$h_1 = x_1 * w(j_1, i_1) + x_2 * w(j_2, i_1) + b_1 \quad (3.17)$$

$$h_2 = x_1 * w(j_2, i_1) + x_2 * w(j_2, i_2) + b_2 \quad (3.18)$$

$$h_3 = x_1 * w(j_3, i1) + x_2 * w(j_3, i_2) + b_3 \quad (3.19)$$

$W(j,i)$ represents the weights of connections between the input node (i) and the hidden neuron (j). The bias parameters, represented as b_1, b_2, b_3, and b_4, are usually set as constant values of one. The output of the hidden layer node is determined by using an activate function (f). As the transfer function, the sigmoid function is widely used. (Hagan, et al., 2014).

$$V_1 = f(h_1) \quad (3.20)$$

$$V_2 = f(h_2) \quad (3.21)$$

$$V_3 = f(h_3) \quad (3.22)$$

Compute the sum of the hidden neuron outputs multiplied by their weights:

$s_0 = v_1 * w(j_1, y) + v_2 * w(j_2, y) + v_3 * w(j_3, y) + b$ (3.23)

$y = f(v_1 * w(j_1, y) + v_2 * w(j_2, y) + v_3 * w(j_3, y) + b_4) = f(s$ (3.24)

The network's output (y) can then be generated by applying the activation function to (s).

Whereas

W(j,y): weight associations between node j and output node y.

f_1, f_2, f_3, and f_4: The sigmoid function is commonly used in transfer functions and has the following form:

$$y = f\left(s_0 = \frac{1}{1 - e^{-s_0}}\right) \quad (3.25)$$

When the training approach is applied to the network, all weights become adjustable parameters. Throughout the training phase, all weights will be modified until a perfect match of input and output forms from the training data set is produced based on the specified minimal errors. (Hagan, et al., 2014).

3.2.3 PID controller

PID controllers are a sort of control loop feedback mechanism that is extensively employed in industrial control systems. The difference among the desired set point and the measured process parameter is represented by the error value. The PID controller aims to minimize error by applying a control value to controlled process. The control value produce via PID controller in time domain is as follows:

$$u(t) = K_p e(t) + K_i \int_0^t e(t)dt + K_d \frac{de(t)}{dt} \quad (3.26)$$

The PID controller's Laplace domain transfer function is given in Equation (3.27), and the U control sign achieved with the PID controller is displayed in Equation (3.28).

$$C_{PID}(s) = K_p + \frac{K_i}{s} + K_d s \quad (3.27)$$

$$U_{PID}(s) = E(s)\left[K_p + \frac{K_i}{s} + K_d s\right] \quad (3.28)$$

In Equation (3.27), the standard PID statement comprises proportional, integral, and derivative operators. K_p denotes proportional gain, K_i denotes integral gain, and K_d denotes derivative gain. E is the error signal in the control signal U_{PID} created by the PID controller given in Equation (3.28). Figure (3.10) below shows the closed loop PID control block diagram in Laplace domain.

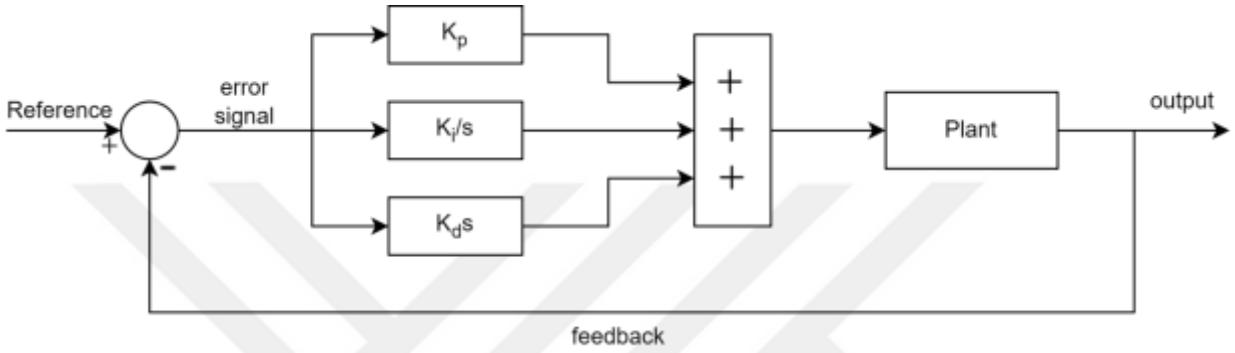

Figure 3.18. Block diagram of a PID controller.

As seen in Figure (3.18), it applies a control signal to the controlled system according to the error signal at the PID controller input. The error sign will be zero when the controlled system output variable reaches the reference value. According to the dynamic behavior of the controlled system, PID controller, P, PI, PD forms are also used.

4. PROPOSED METHOD, RESULTS AND DISCUSSION

In the sections so far, the methods and materials that form the basis of the study are explained. In this section, the method proposed in the thesis study and the results obtained are presented in detail.

Detailed information for PV panels is presented in the above sections. As can be clearly seen from here, the electrical power to be obtained from PV panels directly depends on the solar radiation reaching the panel and the PV panel temperature. In changing radiation and temperature conditions, the MPP point is constantly changing and keeping the PV panel output at the MPP point in each new situation is very important for PV system efficiency. As mentioned in the previous sections, the process of finding and holding the MPP point for the PV panel output power is known as MPPT, and P&O and IC methods are the two most used methods in the literature. In the algorithms of traditional P&O and IC methods, the duty change ratio is constant. This constant duty change rate causes oscillations in the PV output power around the MPP. In this thesis, a method based on changing the fixed value duty ratio in traditional P&O and IC methods is proposed. Thus, it is aimed to improve the performance of traditional P&O and IC methods.

In the proposed method, an ANN was used to estimate the true MPP value in the study. The MPP value estimated by the ANN is used as the reference value for the PID controller. The difference between the ANN prediction and the instantaneous PV panel output is considered as the error value for the PID controller. With the PID controller, it is ensured that the PV panel output of the PID controller is kept around the MPP in any case under changing solar radiation and changing temperature conditions.

The proposed method has been tested with simulation studies in Matlab/Simulink environment. An existing sample Simulink model provided by Matwoks, Matlab Help Center is used. This example includes a 330 kW PV system connected to the grid. There is a step-up DC-DC converter and a 3-phase inverter connected in series to this PV system. The inverter feeds a grid. Details of the experimental setup are presented in the following sections.

The processing steps followed in the study are as follows:

- First of all, MPP points of the PV panel array were determined for different solar radiation and different PV temperatures. A data set was prepared by taking different radiation and temperature values as input parameters and PV output MPP values corresponding to these input parameters as output parameters.

- ANN trainings were carried out using the data set prepared in the second stage. A two-layer ANN structure is preferred.

- In the third step, it is tested whether the trained ANN accurately captures the real MPP values for different irradiance and temperature values.

- In the fourth stage, the PID controller parameters determination (PID tuning) process was carried out to make the difference between the ANN response and the PV output power zero for a constant irradiance and temperature value.

- Finally, the proposed method for different radiation and temperature conditions is compared with traditional P&O and traditional IC MPPT methods, and the results are presented.

4.1. ANN for the proposed method

ANNs are units formed by software or hardware that are based on the modeling of neurons in animals and humans. Artificial neurons are the smallest unit of ANNs. The artificial neuron is made up of inputs, a cell body, parameters that connect the inputs to the cell body, between cells parameters, and an output unit. Input variables to a neuron are multiplied by parameters, and the total of the products is then sent via an activation function. The process of activation is expected to take place within the cell body.

Equation (4.1) represents the output of an artificial neuron.

$$o_i = f\left(\sum_{j-1}^{n} w_{ij}x_j + b_i\right) \tag{4.1}$$

Equation (4.2) represents the parameters update.

$$w(n) = w(n-1) + \Delta w(n) \tag{4.2}$$

In (4.1), *o* stands for cell output, *x* stands for input variable, and *b* stands for bias. The activation function is represented by (*f*). Parameters are represented by *w* in Equations (4.1) and (4.2). *w* represents the number of parameters change in Equation (4.2), and this formula is discovered using a learning method.

A limited number of neurons combine to produce an ANN. An ANN architecture can be constructed with either a single layer or multiple layers. Artificial neural networks (ANN) have the capability to develop and generalize. The majority of learning is accomplished by updating

the ANN parameters. Several learning algorithms have been created in the literature for the updating of weights, i.e. for the learning process. There are three types of learning algorithms: supervised, unsupervised, and reinforcement. An additional benefit of ANNs is their ability to handle incoming data in parallel due to their parallel nature. This allows for the teaching of quick reactions.

ANN design and learning techniques may be customized for each application. The two-layer ANN design was selected for this research. Figure (4.1) depicts the applied structure off ANN.

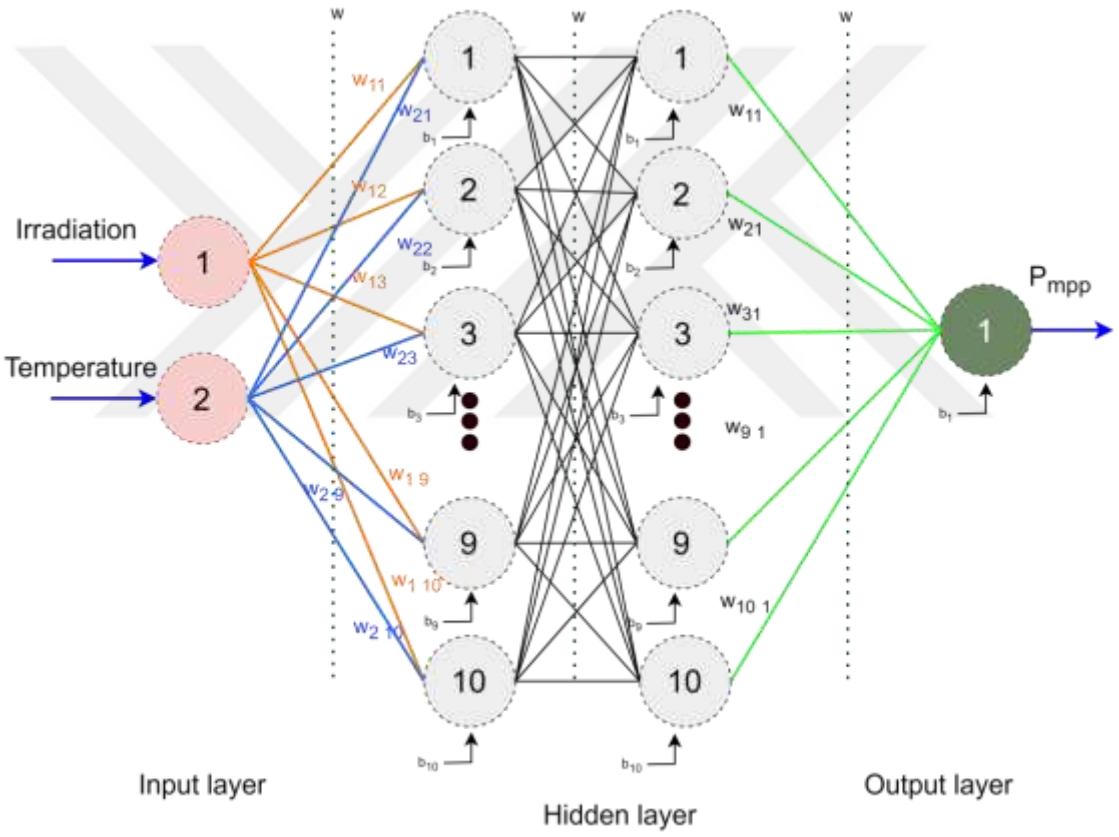

Figure 4.1. Single-layer ANN model in the study.

Each hidden layer has ten cells. The learning algorithm was the Levenberg-Marquardt (LM) technique, the tangent sigmoid activation function was utilized in the cells in the hidden layers, and the Purlin activation function was used in the output layer. Equation (4.3) performs the LM technique. w is the weight vector, I is the unit matrix, μ is the learning parameter, and J is the Jacobian matrix representing the output error in Equation (4.3).

$$w(n) = w(n-1) - (J_n^T J_n + \mu_n I)^{-1} J_n^T E_n \tag{4.3}$$

Nonlinear problems, curve fitting, estimation, and prediction are all common applications for ANNs. In this paper, ANN is applied to estimate the MPP value of a PV array provided radiation and temperature conditions. Figure (4.2) illustrates the proposed approach in the research.

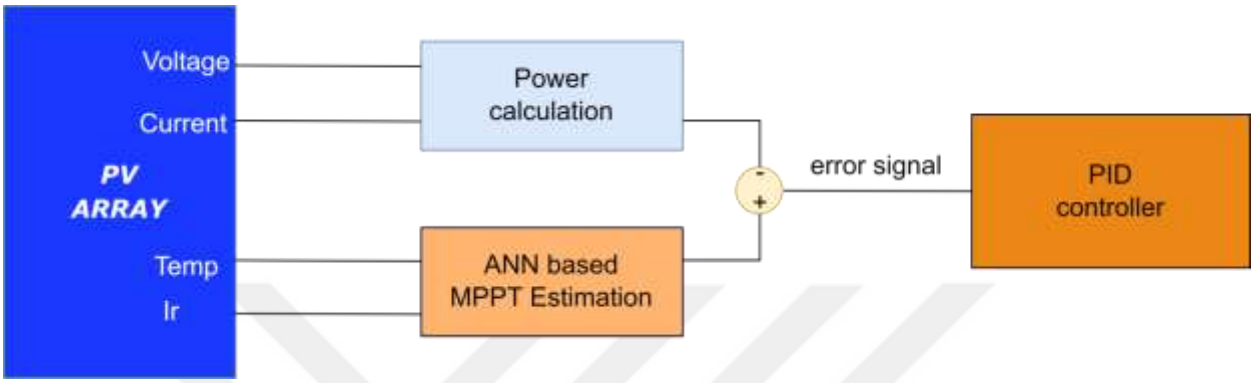

Figure 4.2. MPPT control structure proposed in the study.

The ANN's parameters in Figure (4.2) are solar radiation and PV temperature. As a result, the ANN will be able to determine the maximum power required from the PV array for each irradiance and temperature value. The maximum power value discovered by the ANN for each condition is utilized as a reference value throughout the research. An error (e) value is calculated by taking the difference between the MPP value estimated by the ANN and the instantaneous power of the PV array. The error value is tried to be reduced to zero by using the PID controller. The control signal obtained with PID is used as the duty change ratio in conventional P&O and conventional IC MPPT methods. A variable duty change ratio is obtained for each new radiation and temperature. Thus, as the MPP point is approached, the duty change ratio is reduced and the oscillation ratio in the PV output power is also reduced.

As in all other control applications, PID controller parameters K_p, K_i and K_d values must be determined in order to obtain an effective performance. This topic is explained in the next section.

4.2. PID controller design

PID controller design (tuning) refers to the process of finding the PID controller's K_p, K_i, and K_d gain coefficients. For PID tuning, several analytical, soft computing, and metaheuristic approaches are proposed in the literature. Metaheuristic algorithms are inspired by the natural behavior of animals who collaborate to solve food and defensive problems. Metaheuristic algorithms include the Genetic Algorithm (GA), Particle Swarm Optimization (PSO), Artificial Bee Colony (ABC), and Ant Colony Optimization (ACO). Swarm intelligence supports PSO, ACO, and ABC. GA is focused on growth. GA does not require knowledge of the system's

mathematical model, just input-output data is required. As a result, it is a popular way for dealing with difficult situations. It can deal with significant parameter uncertainty. Another benefit of GA is that, while it's computing time is comparable to that of the PSO method, it is twice as quick as the ABC algorithm (Bagis and Senberber, 2017).

The Genetic Algorithm (GA) was chosen for this research, allowing for practical and high-quality outcomes. The Integral of Time-Weighted Absolute Error (ITAE) presented in Equation (4.4) is utilized as the fitness function for GA. The value of the error in Equation (4.5), is the difference between the MPP at 1000 W/m^2 irradiance, 25°C and the PV system output power. PID controller gains were calculated by plugging this error value into Equation (4.4) and reducing it with GA optimization. Figure (4.3) depicts the tuning of PID K_p, K_i, and K_d gains using the GA optimization flowchart. K_p =1, K_i = 0.0057, and K_d = 0.0001were achieved as a result of GA optimization.

$$fitness(ITAE) = \int t|e(t)|dt \tag{4.4}$$

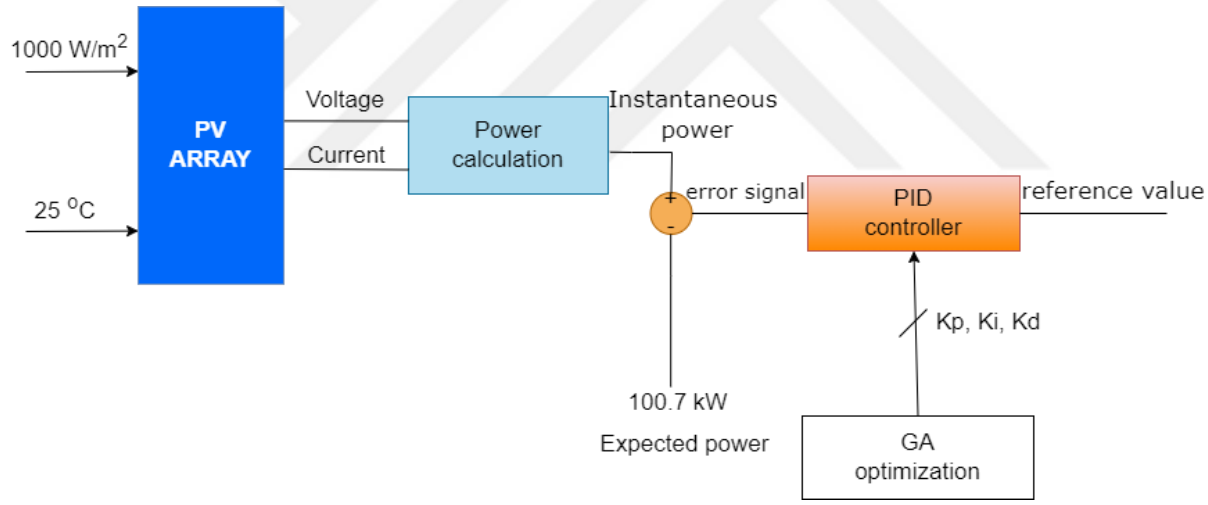

Figure 4.3. PID tuning based on GA optimization block diagram.

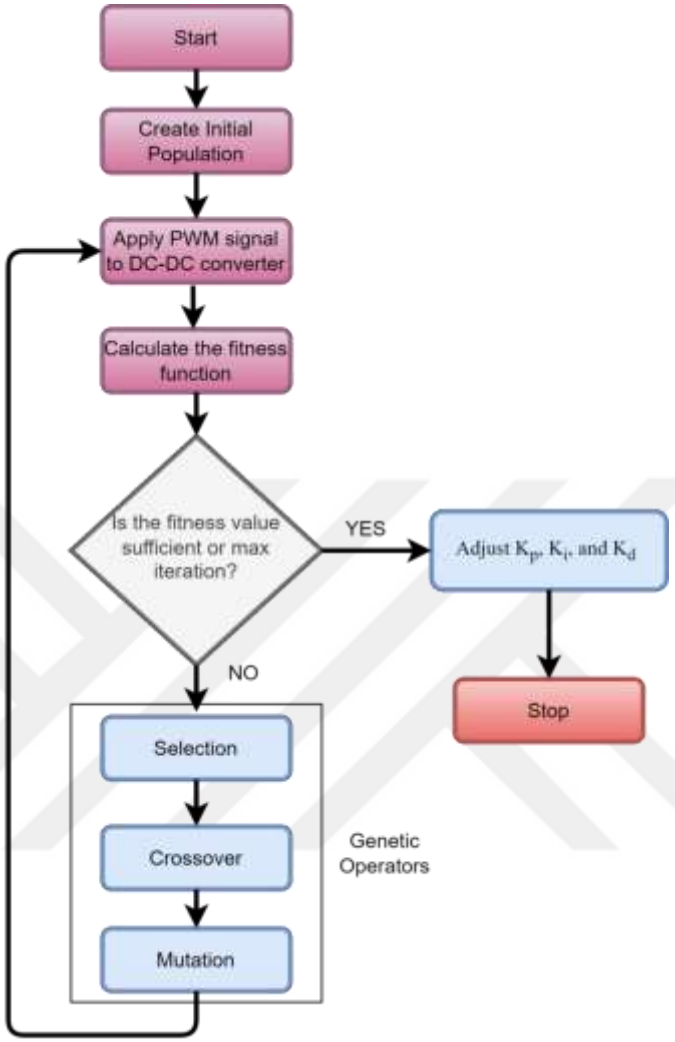

Figure 4.4. Flow chart of PID tuning using the GA optimization.

4.3 Training of the ANN at different Temperature and Irradiation

The ANN's inputs are instantaneous solar radiation and PV temperature, as shown in the ANN structure in Figure (4.1). Based on these two immediate variables, ANN calculates the instantaneous MPP value. The high estimate accuracy is determined by the ANN's training procedure. An adequate amount of input and output data is required for ANN training. The MPP output value was acquired for (5105) different radiation and temperature input values in the research, as well as the ANN training data set. The irradiance range of 0-1000 W/m^2 and the temperature inducing value range of -55 degrees ^{o}C to +55 degrees ^{o}C were used when producing the data set. Equations (4.5) and (4.6) are used to create random values in these intervals. In this case, rand (1) is a function that creates a random value between 0 and 1.

$$IR = 1000 \times rand(1) \tag{4.5}$$

$$TEMP = -55 \times rand(1) + 55 \times rand(1) \quad (4.6)$$

This training set was used to train ANN. 3573 (%70) samples were utilized for training, 766 (%15) samples for validation, and 766 (%15) samples for testing. Table (1) contains 20 samples from the training set, and Figure (4.5) displays complete input-output data.

Table (1). Some training data samples.

Irradiance W/m^2	**Temperature °C**	**MPP (kW)**
42.8234	-16.7092	4.4850
930.6002	16.4435	95.6983
20.9586	-18.9415	2.1601
518.2959	26.7803	51.2859
615.3479	-22.54896	69.3971
994.9164	41.3357	94.7287
395.9904	-45.9427	45.1995
667.1600	2.2690	71.1291
792.6156	11.2611	82.6053
907.9813	12.1968	94.4738
126.4463	-3.1952	13.1580
830.9913	-13.0234	92,3235
863.0336	8.0572	90.7971
718.3575	-10.0591	79.1529
188.6699	-28.1340	21.1179
782.4692	4.0493	83.1597
695.4217	20.3734	70.5170
66.6428	-44.9071	7.5016
659.3253	-4.0405	71.4705
623.9580	31.7578	61.0367

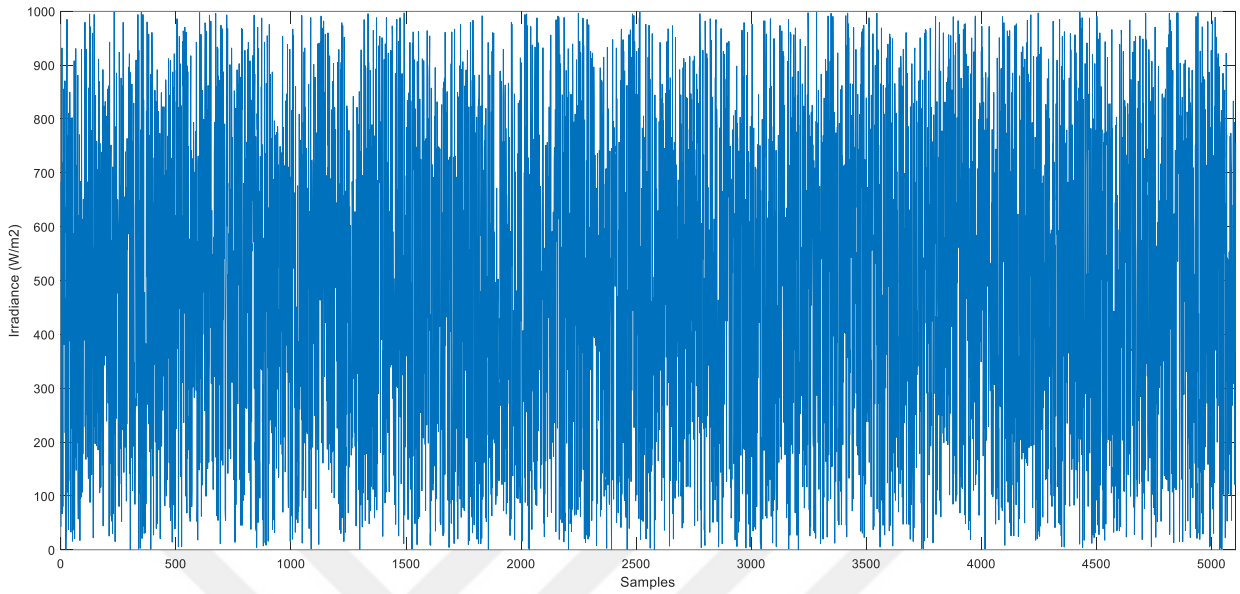
Irradiance (W/m2)
Samples
0
100
200
300
400
500
600
700
800
900
1000
0
500
1000
1500
2000
2500
3000
3500
4000
4500
5000

(a)

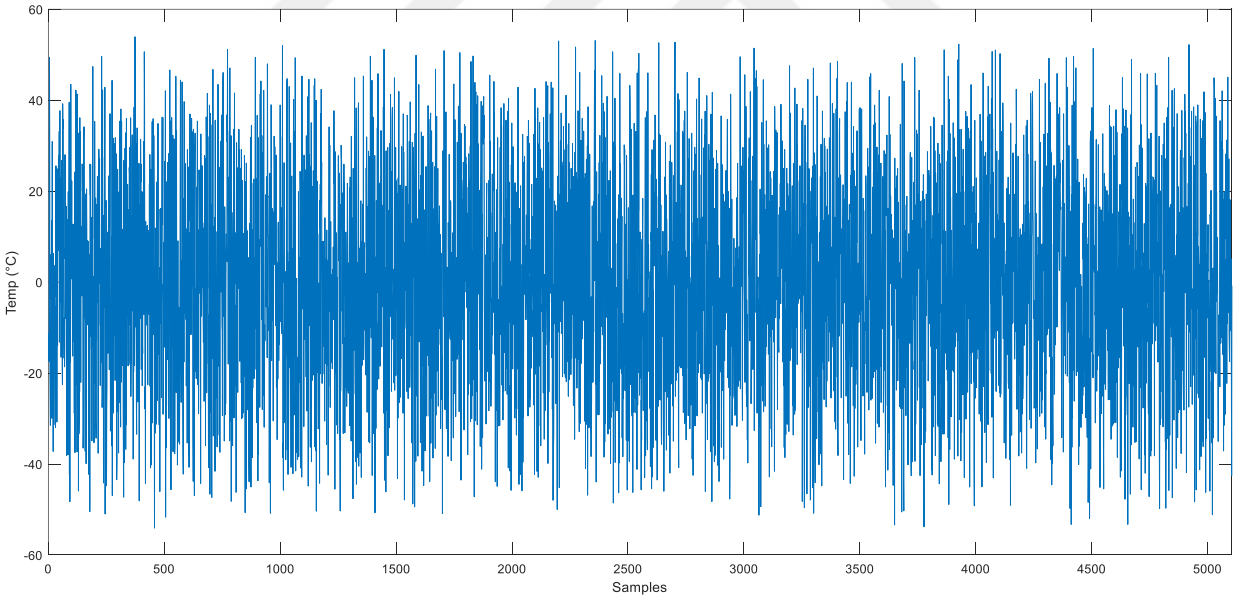
Temp (°C)
Samples
60
40
20
0
-20
-40
-60
0
500
1000
1500
2000
2500
3000
3500
4000
4500
5000

(b)

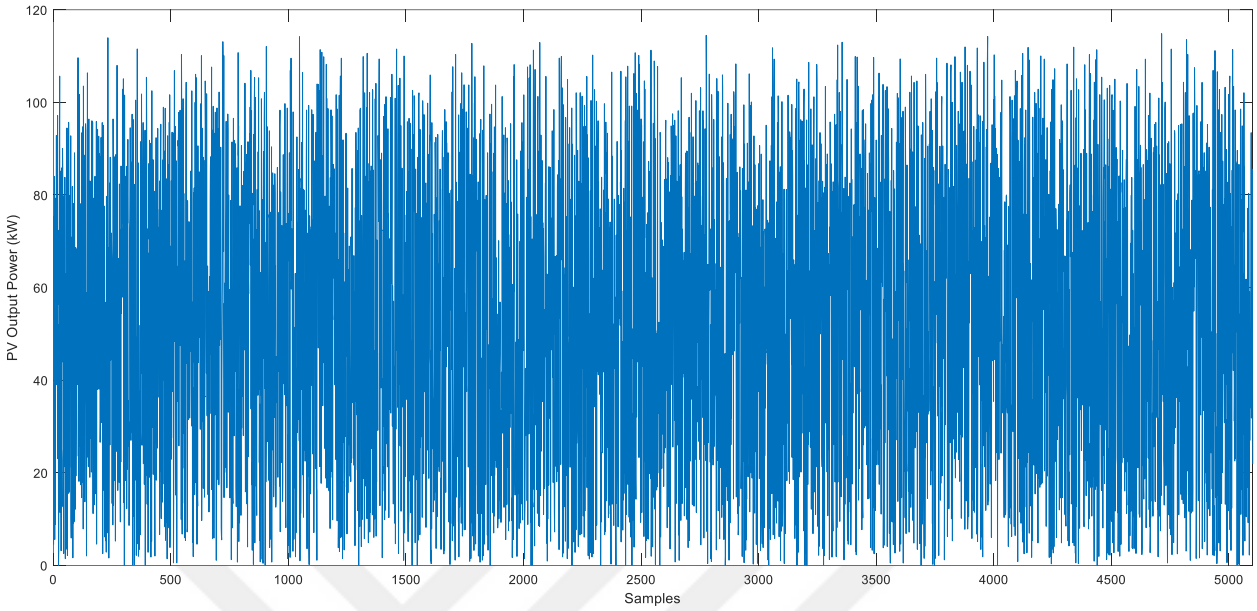

(c)

Figure 4.5. The training data set. (a). Irradiance. (b). Temperature. (c). Maximum power point.

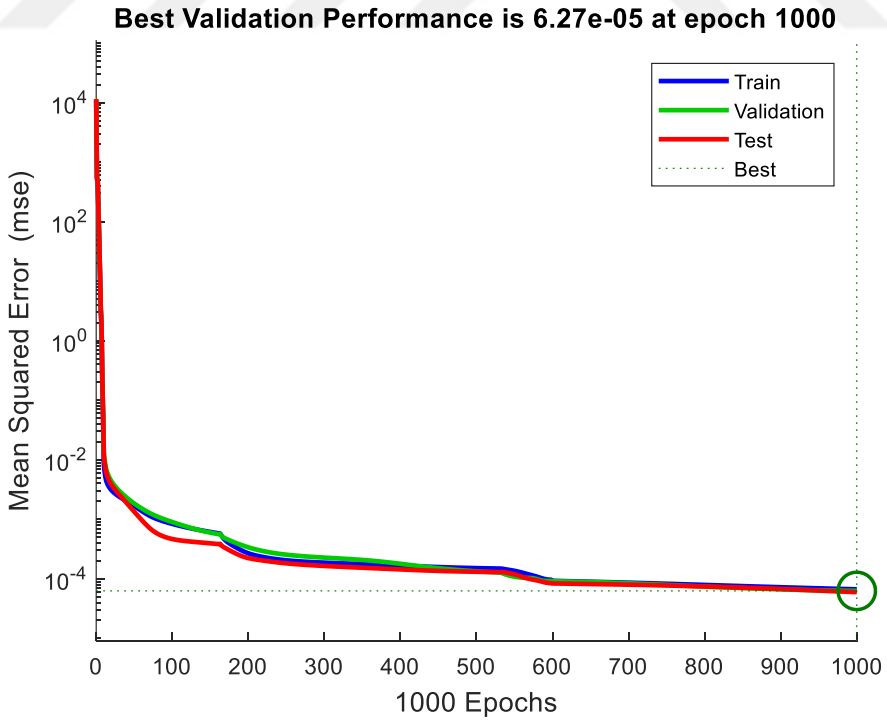

(a)

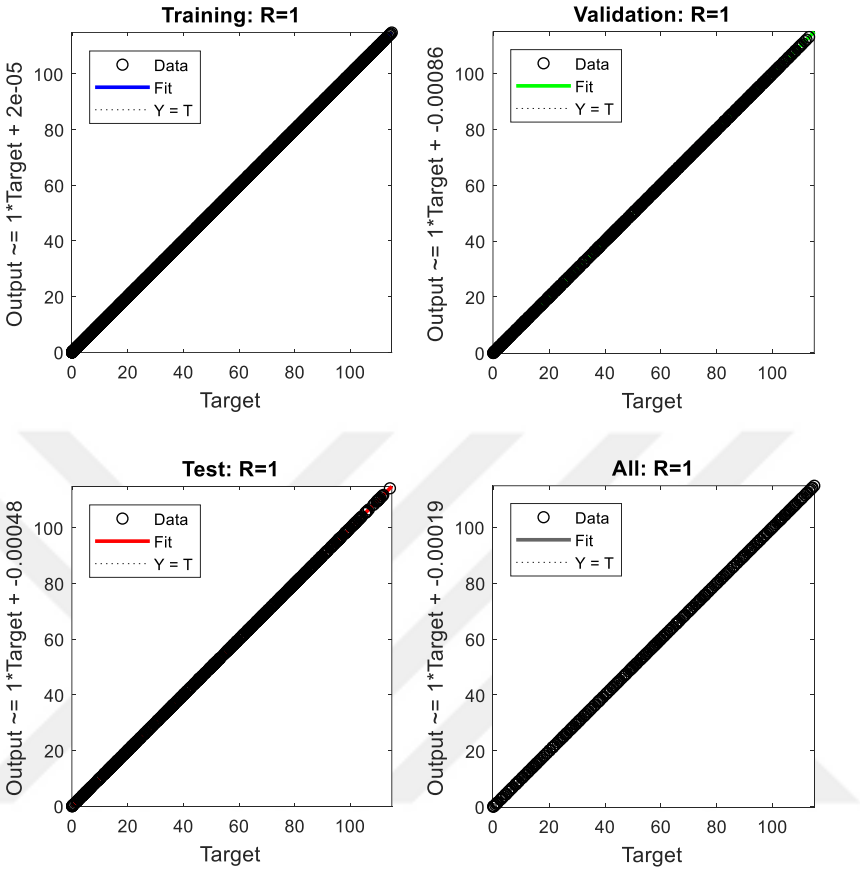

(b)

Figure 4.6. ANN's training graphs. a. Performance, b. Regression.

Figure (4.6) depicts training performance and regression curves. As shown in Figure (4.6), the training lasted 1000 epochs, and the performance value decreased to 6.27×10^{-5} as a result of the training, while the regression value was increased to 1. Here, at the end of 1000 epochs, the train, validation and test curves dropped to 6.27×10^{-5} together and all the data were collected on the regression curve, showing that the performance of the training was very good.

4.4 Simulation studies

The study was carried out as a simulation study on Matlab/Simulink. The blocks used in the study are shown in Figure 4.7. In the study, a PV array generating 100.7 kW at 1000 W/m^2 and 25 °C was used, using SunPower SPR-305E-WHT-D panels arranged in 5 series and 66 parallel (330 units). The PV output is connected to a grid by a step-up DC-DC converter and a 3-phase inverter. The PWM switching frequency of the DC-DC converter is 5 kHz, and the inverter input voltage level is 500V. As seen in Figure (4.7), there are 5 basic block groups.

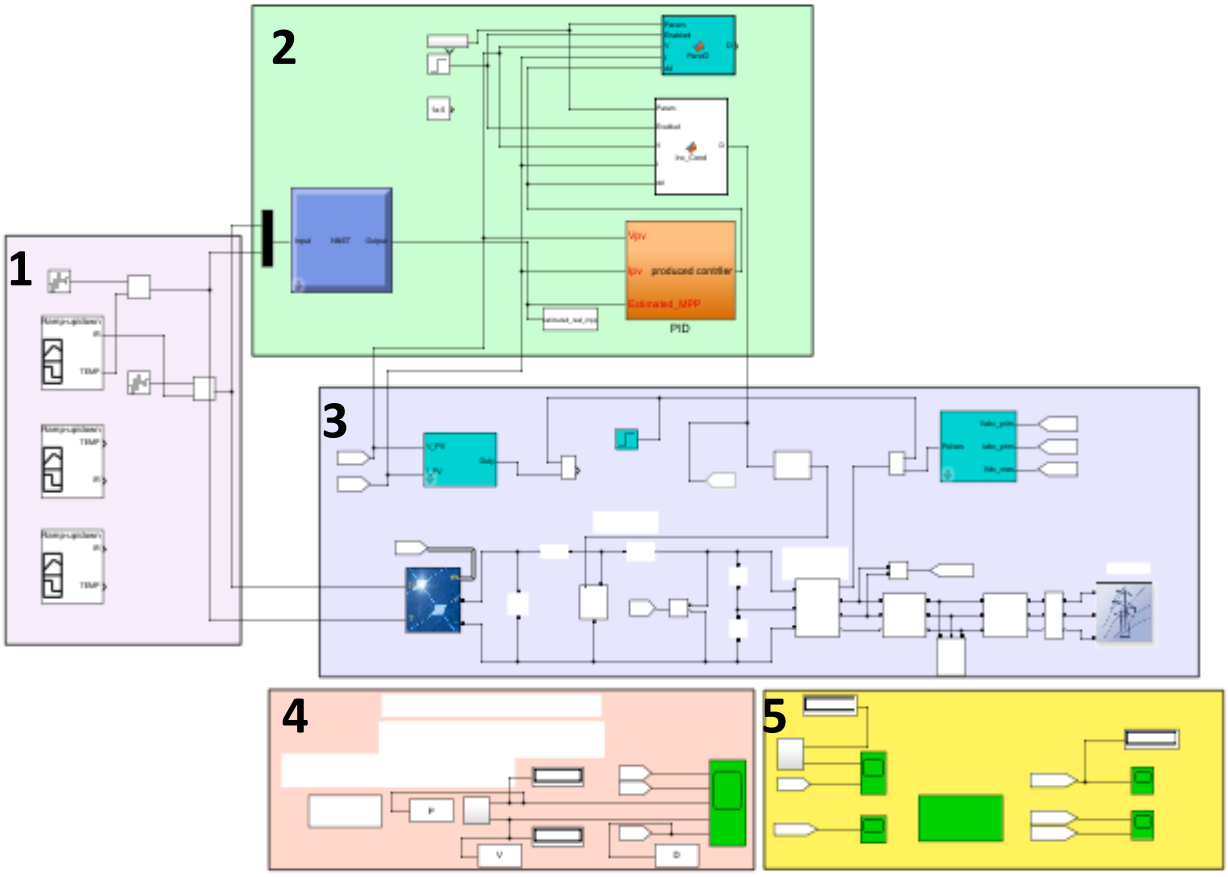

Figure 4.7 Overall PV array Simulink model of grid-connected system. (Matwoks, Matlab Help Center.)

In the first block group there are solar radiation and temperature signal generators, in the second group there are ANN and P&O, IC and proposed PID MPPT controller blocks, in the third block group there are PV array, DC-DC converter, inverter and grid connection. The fourth and fifth groups include measurement and monitoring blocks. In Figure (4.8.a), signal generators are used to represent different environmental conditions (radiation and temperature). The radiation and temperature graphs obtained by using these generators in the study are presented in Figure (4.8.b).

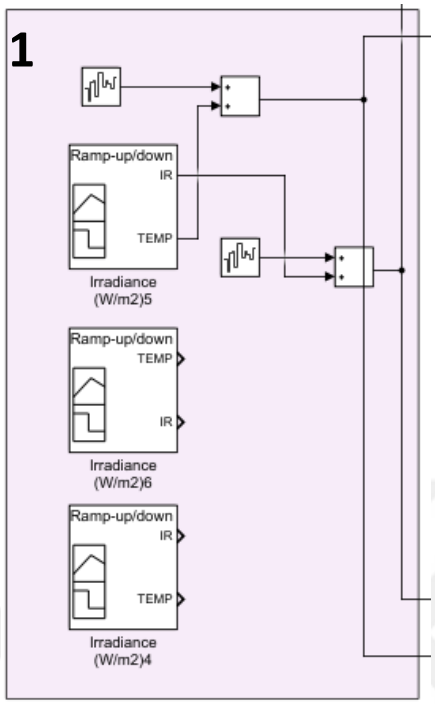

(a)

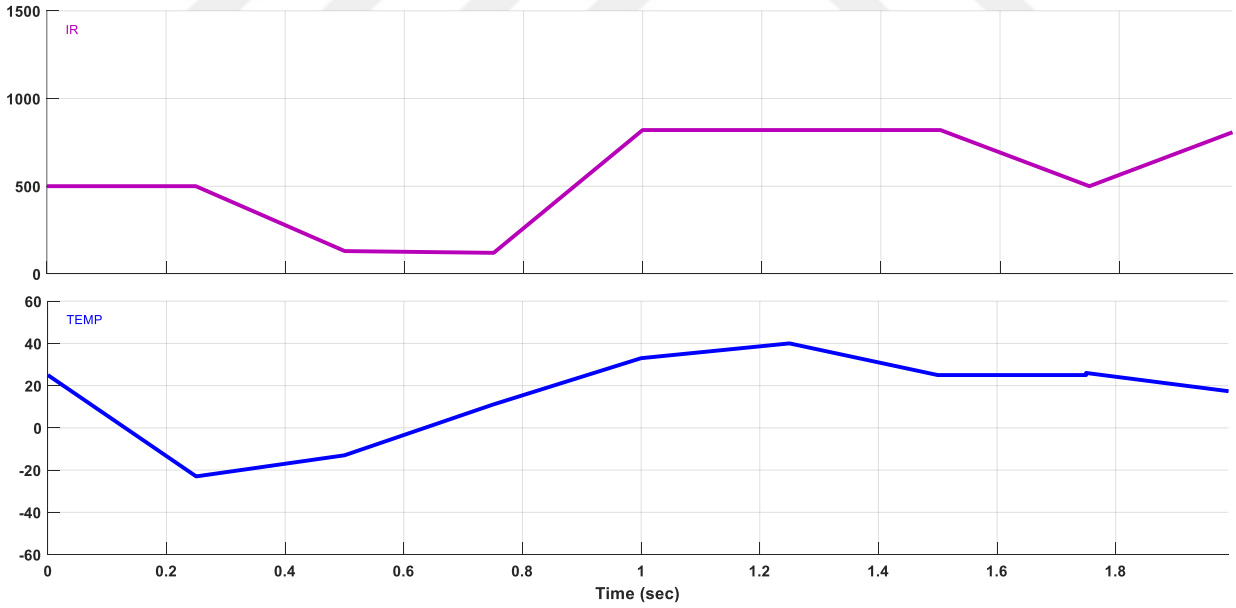

(b)

Figure 4.8. Different temperature and irradiance conditions. a. Generator blocks. b. Temperature and irradiance graphs.

Figure (4.9) shows the ANN, P&O, IC and recommended PID MPPT controller blocks. Here, the solar radiation and temperature value, which are the two inputs of the ANN, are obtained with the signal generators in Figure (4.8). As seen in Figure (4.9), the ANN output (named Estimated_MPP on the PID block) goes to the proposed PID MPPT controller block. The output of the proposed PID MPPT controller block is applied as the input parameter named "*Produced_controller_sign*" to the blocks in which traditional P&O and conventional IC methods are run. Here the " *Produced_controller_sign* " stands for "delta of duty". In this case, with the proposed method, an adaptive MPPT control structure is obtained by obtaining different duty change rates for varying temperature and radiation values. The internal structure of the proposed PID MPPT controller block is explained in detail in the Figure (4.9.b).

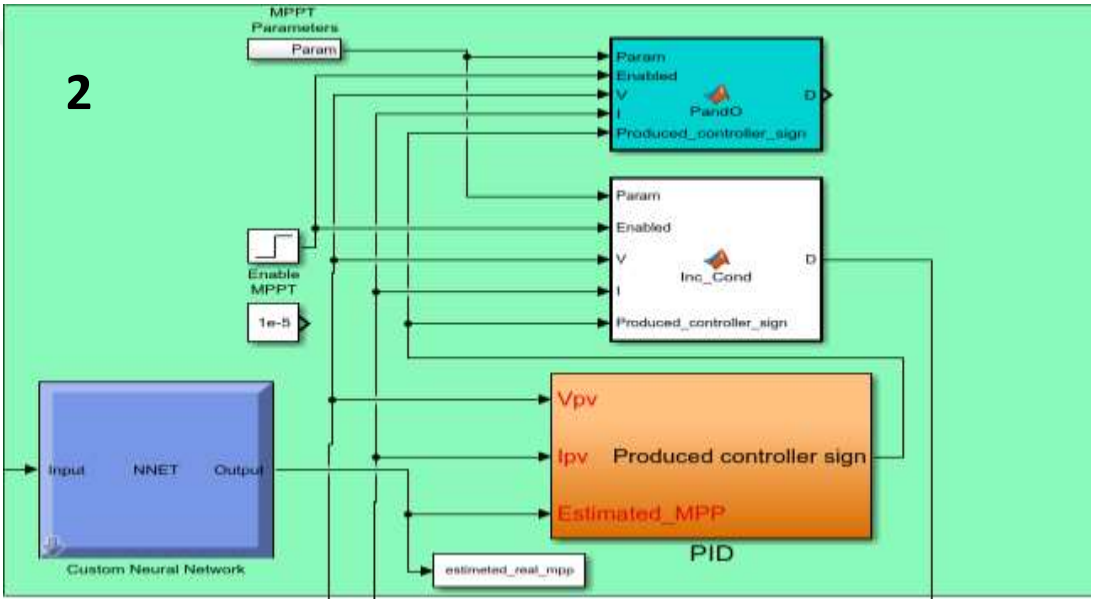

(a)

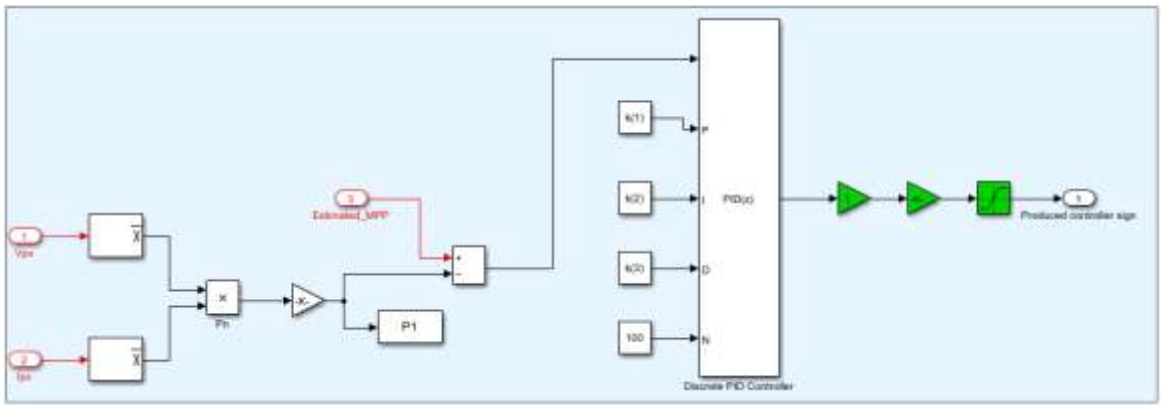

(b)

Figure 4.9. a. ANN and MPPT controller blocks. b. Internal structure of the proposed PID MPPT controller block.

As seen in Figure (4.9.b), the PV array current and voltage are read by sensors and their average values are taken. Thus, small changes are filtered out. By multiplying these two values, the instantaneous value of the PV array is calculated. Then, the error value is obtained by taking the difference between the MPP value estimated by the ANN and the calculated instantaneous PV power. This error value is reduced to zero with the PID controller. The PID control output sign is the *dd* sign in Figure 4.9.a. Here, the parameters $k(1)$, $k(2)$ and $k(3)$ are the K_p, Ki and K_d values determined by optimization, respectively. Again here the "K" gain value is 1/10000. PV array connected to DC-DC Boost converter, 3 phase inverter and grid-connected system are detailed shown in the Figure (4.10).

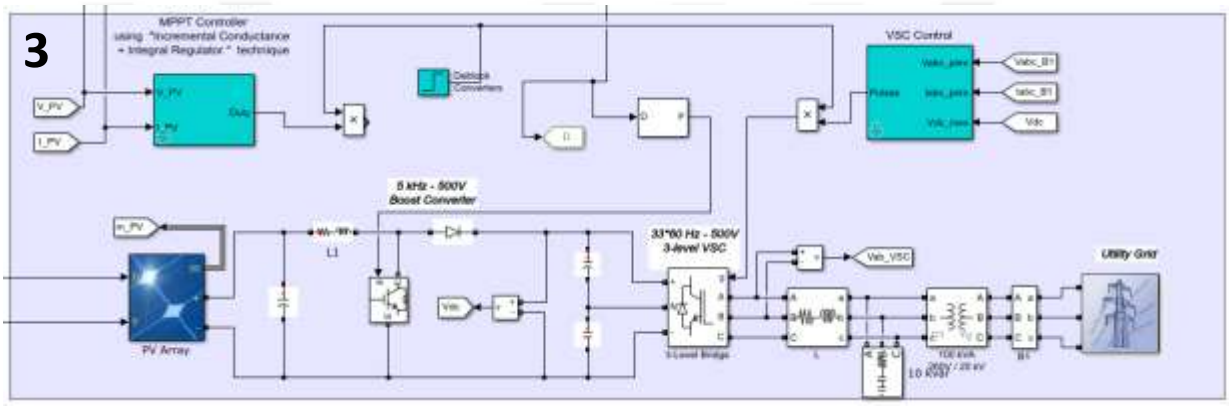

Figure 4.10. Grid-connected PV array. (Matwoks, Matlab Help Center.)

Figure (4.11(a)). Shown the measurements blocks for produced power, operated voltage and duty cycle and general information about the system. Figure (4.11(b)) shown some important blocks for the working of the system.

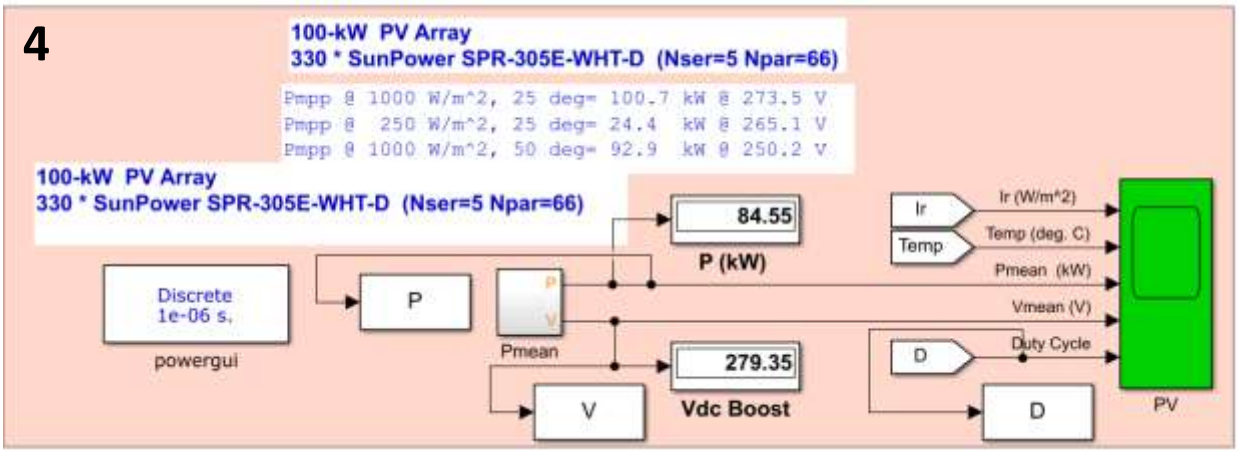

(a)

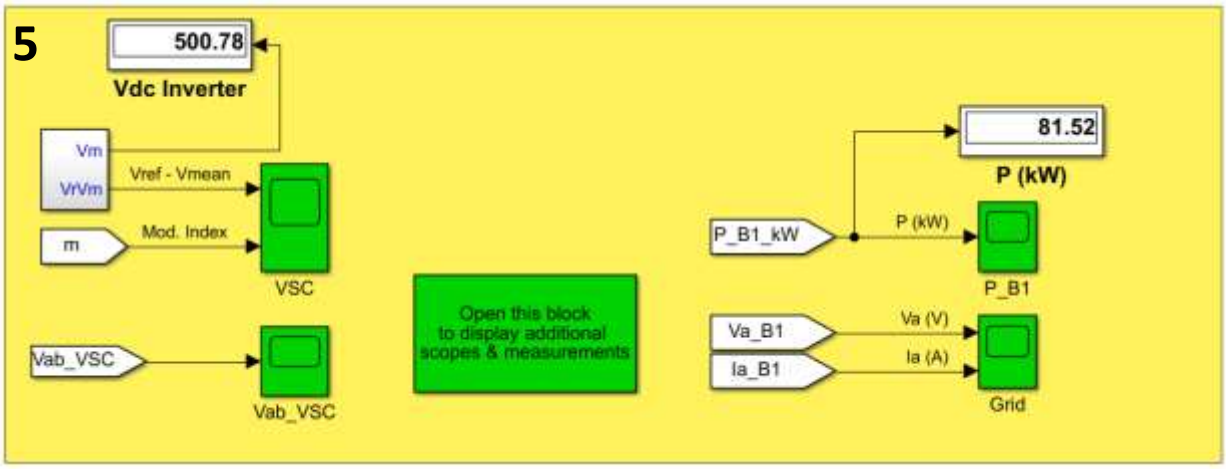

(b)

Figure 4.11. Measurement blocks. (a) Power, duty cycle and operated voltage. (b) Some important blocks for the system. (Matwoks, Matlab Help Center.)

The following pages show the simulation results based on Matlab/Simulink at varying temperatures and irradiation conditions. The results here were obtained according to the values in the radiation and temperature graph in Figure (4.8). The proposed method is compared with traditional P&O and traditional IC methods at these given values. The comparison is made in terms of PV array output power, duty sign and PV output voltage. The results obtained are Figures (4.12), (4.13) and (4.14).

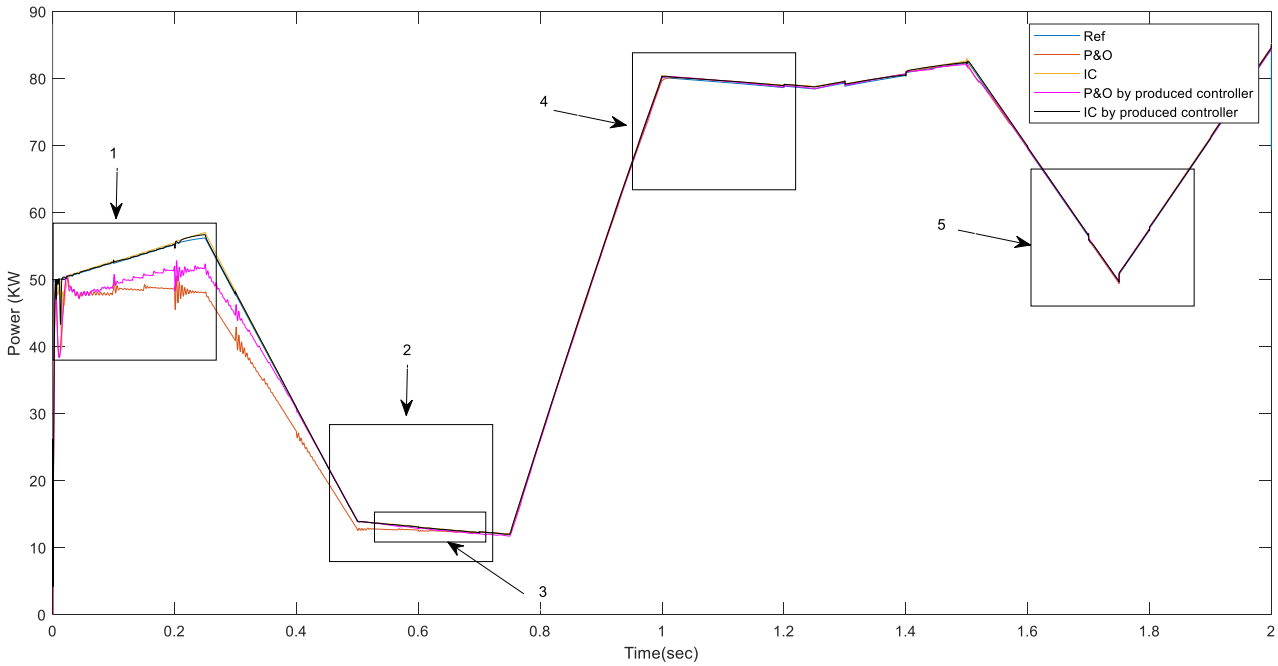

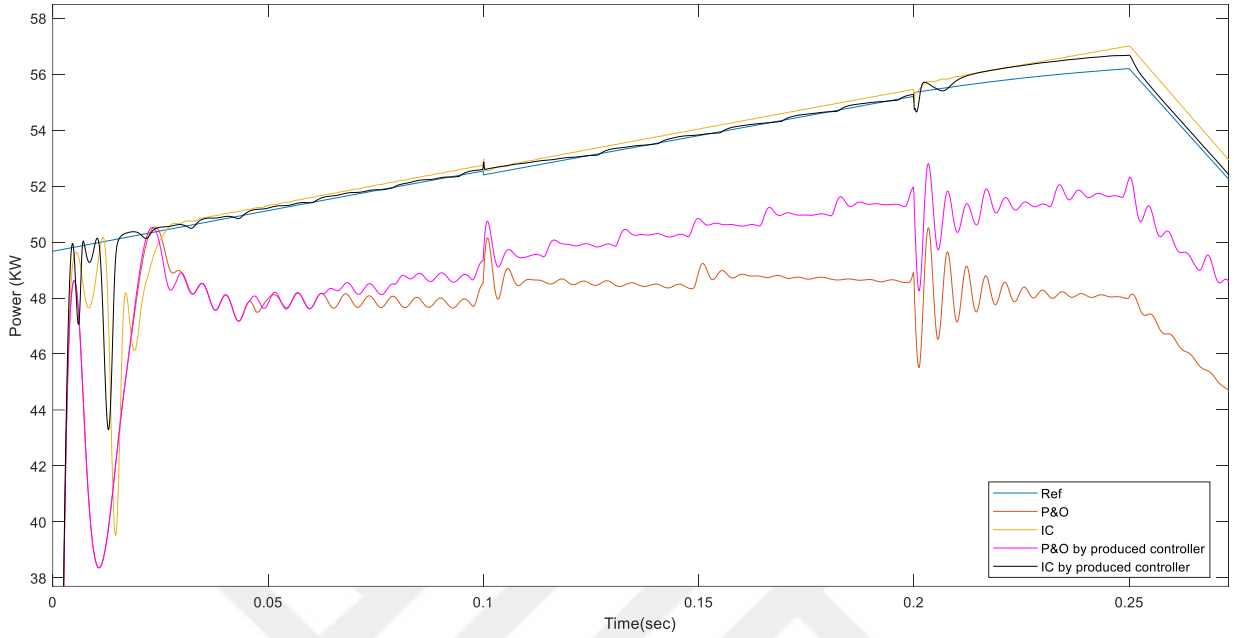
Power (KW
Time(sec)
Ref
P&O
IC
P&O by produced controller
IC by produced controller

(1)

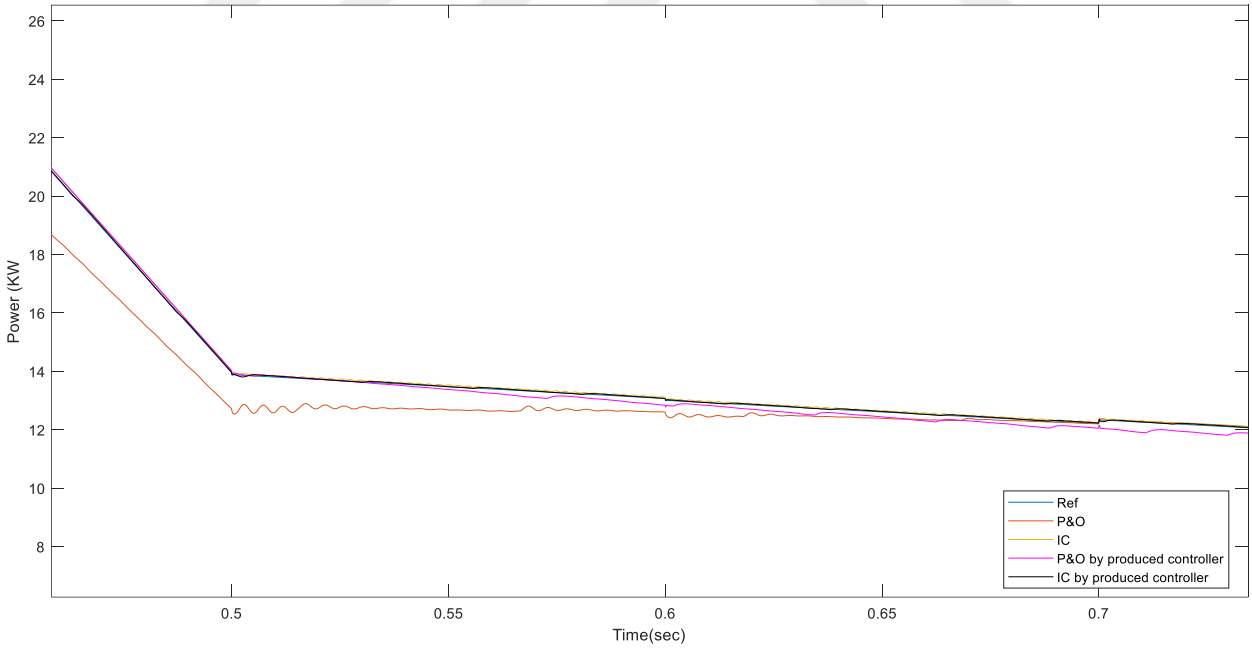
Power (KW
Time(sec)
Ref
P&O
IC
P&O by produced controller
IC by produced controller

(2)

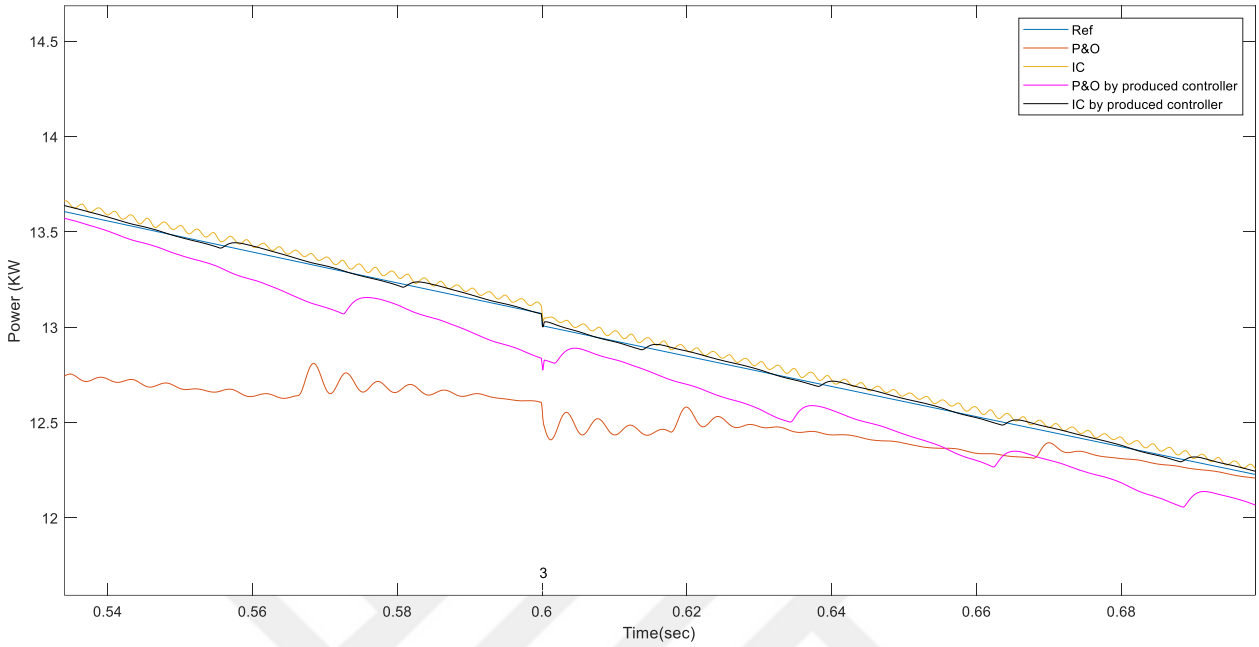
Ref
P&O
IC
P&O by produced controller
IC by produced controller
Power (KW
Time(sec)
14.5
14
13.5
13
12.5
12
0.54
0.56
0.58
0.6
0.62
0.64
0.66
0.68
3

(3)

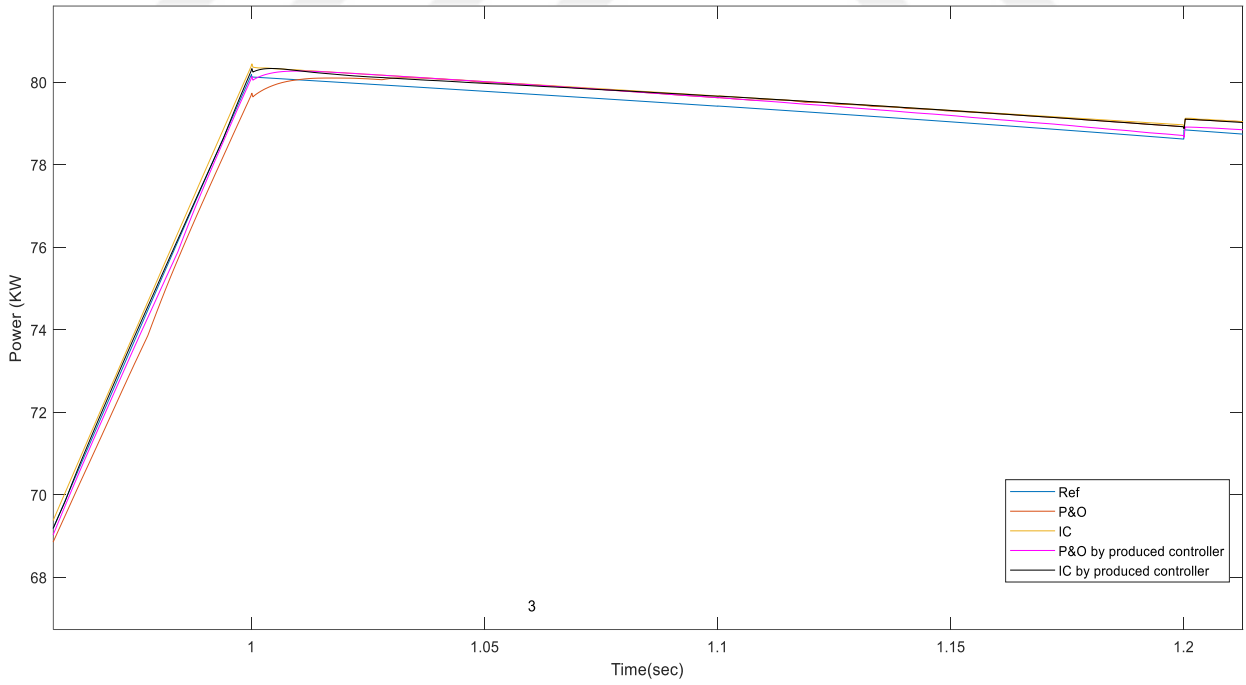
Ref
P&O
IC
P&O by produced controller
IC by produced controller
Power (KW
Time(sec)
80
78
76
74
72
70
68
1
1.05
1.1
1.15
1.2
3

(4)

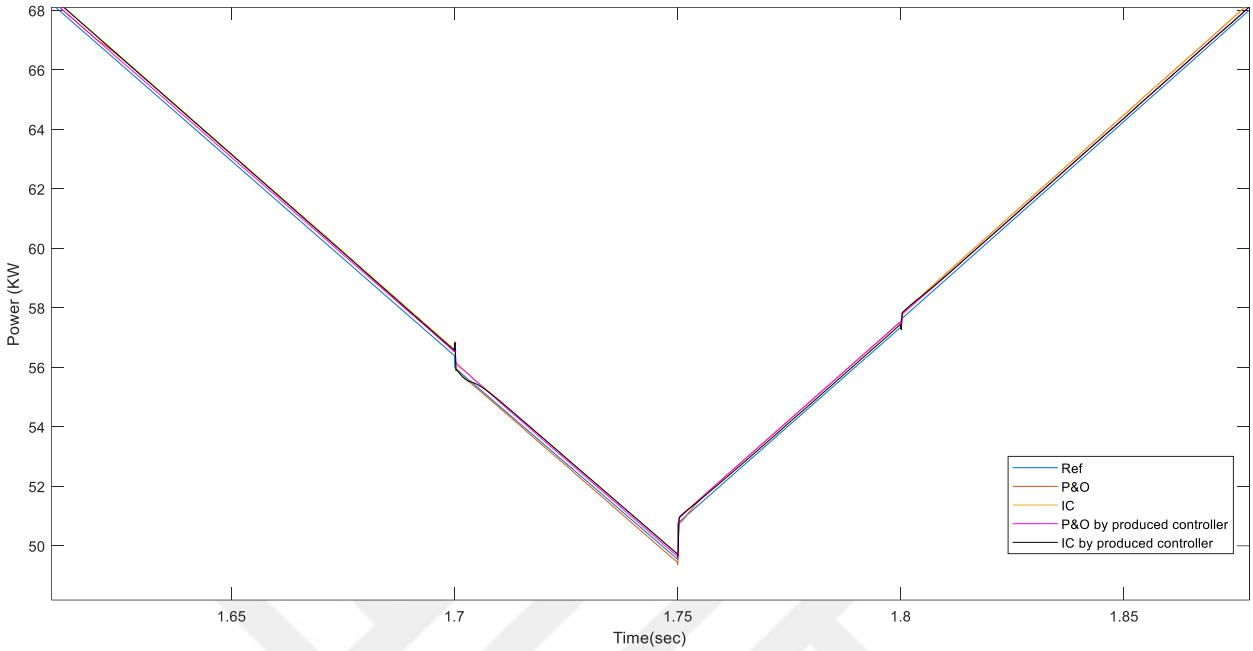

(5)

Figure 4.12. Comparison of conventional and suggested methods method in terms of PV power.

As seen in Figure (4.12), it is shown that the IC method makes it possible to obtain a better PV output power than the P&O method. Also around MPP crap, there is more power fluctuation than traditional methods, especially at low power levels. In the proposed method, the power fluctuation rate is negligible. In addition, a significant power increase can be obtained in the P&O method supported by the proposed method compared to the traditional P&O method.

Figure (4.13) shows the comparison of the proposed method with traditional methods in terms of duty ratio. It can be clearly seen here that a less oscillating duty signal can be obtained with the proposed method. This will reduce the switching frequency in the DC-DC converter and therefore reduce the switching losses. This will also contribute to a longer lifetime of the DC-DC converter and to reduce the harmonic generation.

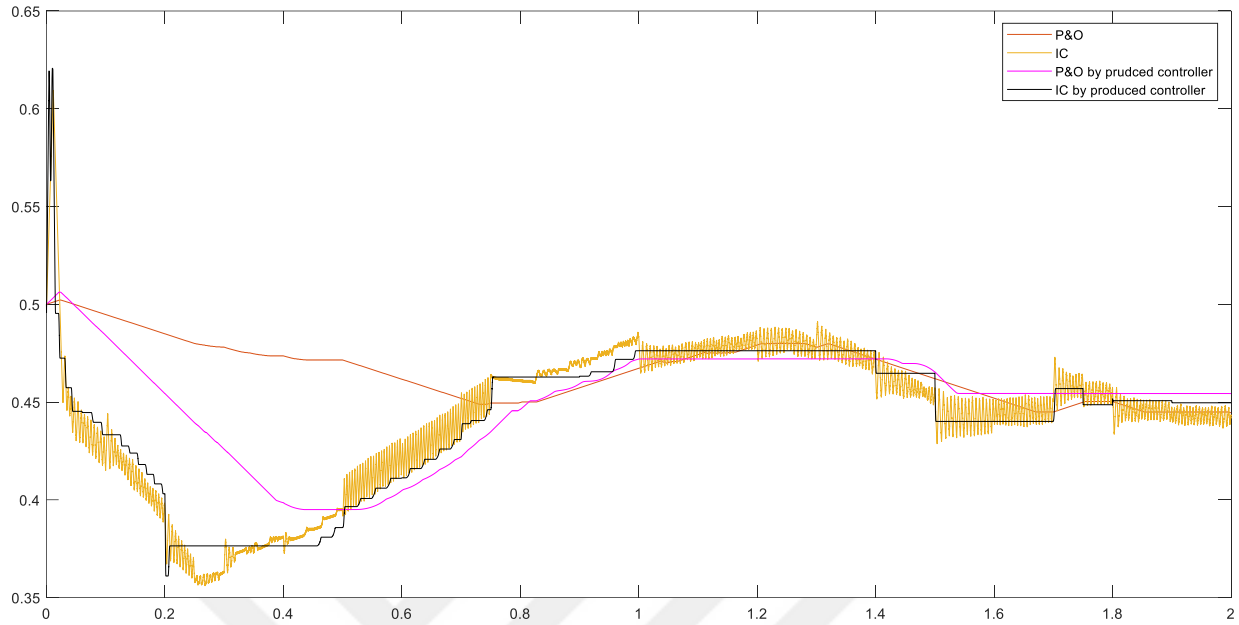

Figure 4.13. Comparison of suggested method and conventional methods in terms of duty ratio.

In Figure (4.14), the proposed method is compared with other conventional methods in terms of output voltages of the PV array. As can be seen here, there is a serious voltage fluctuation in conventional methods, especially in the IC method, depending on the duty ratio.

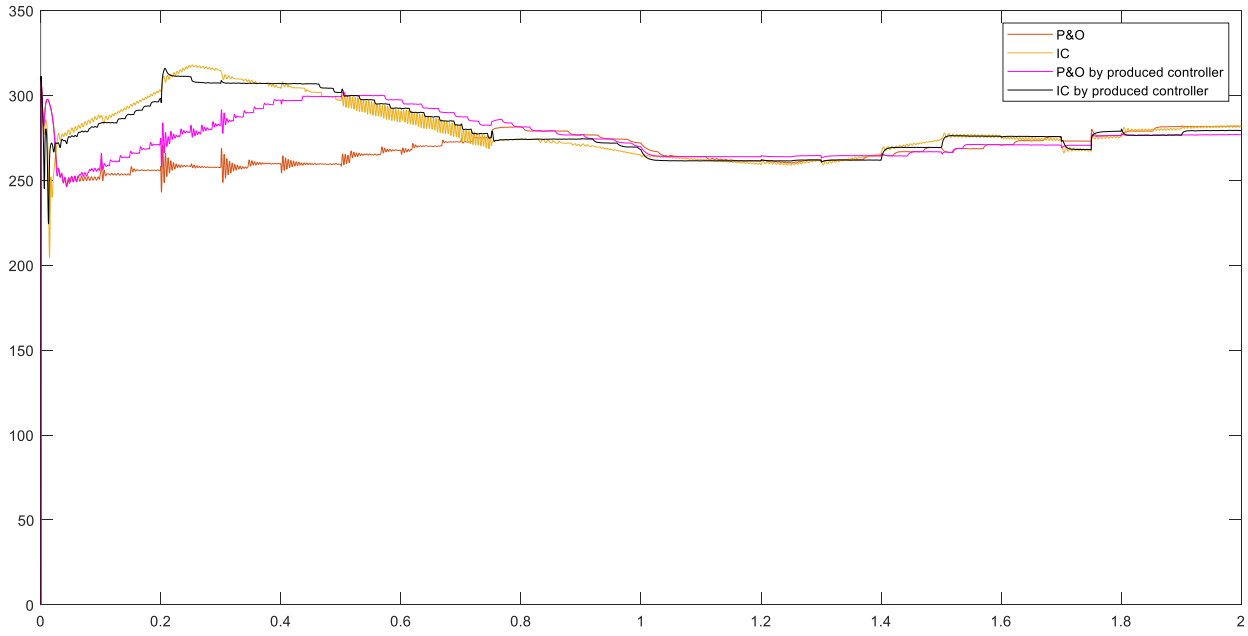

Figure 4.14. Comparison between P&O, IC, P&O by suggested method and IC by suggested method in terms of voltage at different temperatures and irradiances.

The outputs of the suggested controller simulations were compared. The results show less oscillation, more power, and better voltage as compared to the P&O and IC approaches. It generates more power and is more precise when operating at MPP than the previously stated technique.

5. CONCLUSION

PV solar systems are important renewable energy sources as they do not release harmful chemicals into the environment and are relatively endless. MPPT control approaches are utilized to optimize the power output of PV solar systems in order to enhance their efficiency.

In this thesis, the development of an ANN and PID controller-based method for MPPT is focused. In the proposed method, ANN uses instantaneous solar radiation and PV panel temperature as input and finds the MPP value that should be according to these input values. The difference between the ANN output and the instantaneous output value of the PV array is used as the error value of the PID controller. The PID output is used as a reference value for traditional P&O and IC methods. Thus, a reference value that changes according to varying radiation and temperature values is obtained.

Instant solar radiation and PV panel temperature values were used for the training of ANN. The irradiance range of 0-1000 W/m2 and the temperature inducing value range of -55 degrees ^{o}C to +55 degrees ^{o}C were used when producing the data set. Thus, real environmental conditions were tried to be obtained. 5105 pieces of data were used in the ANN training set. This training set was used to train ANN. 3573 (70%) samples were utilized for training, 766 (15%) samples for validation, and 766 (15%) samples for testing.

Genetic Algorithm (GA) was chosen to find the optimal values of the K_p, K_i and K_d parameters of the PID controller. ITAE is used as the optimization fitness function. For error value in ITAE fitness function, 1000 W/m^2 irradiance, difference between MPP and PV system output power at 25°C is used.

In the study, a 100 kW PV array was connected to the electricity grid by means of a boost DC-DC converter and an inverter, and simulation studies were carried out for different solar radiation and PV panel temperature values. In compared to traditional P&O and IC, the suggested technique outperforms them in terms of output power, voltage, and duty cycle.

6. REFERENCES

Abdelwahab, S. A. M., Hamada, A. M., & Abdellatif, W. S. (2020). Comparative analysis of the modified perturb & observe with different MPPT techniques for PV grid connected systems. International journal of renewable energy Research, 10(1), 55-164.

Ahmed, Emad M., et al. (2022). Enhancement of MPPT Controller in PV-Bes System Using Incremental Conductance along with Hybrid Crow-Pattern Search Approach Based ANFIS under Different Environmental Conditions. Sustainable Energy Technologies and Assessments, vol. 50, p. 101812.

Albarbar, A. H. Natsheh, E. M., & Natsheh, A. R., (2014). An automated tool for solar power systems. Applied Solar Energy, *50*, 221-227.

Badamchizadeh, M. A., Sedaghati, F., Nahavandi, A., Abedinpour Fallah, M. & Ghaemi, S., (2012). PV maximum power-point tracking by using artificial neural network. Mathematical Problems in Engineering, 2012.

Bagis, A and Senberber, H. (2017). ABC algorithm based PID controller design for higher order oscillatory systems. Elektronika Ir Elektrotechnika 23(6): 3–9.

Bhatnagar P. &, Nema R. K., (2013). Maximum power point tracking control techniques: State-of-the-art in photovoltaic applications, Renewable and Sustainable Energy Reviews 23, 224–241.

Bindner, H. Hansen, L. H., W Sørensen, P. E., &. Hansen, A. D., (2001). Models for a stand-alone PV system. (Report No. 87-550-2774-1). Denmark: Technical University of Denmark, Frederiksborgvej.

Bohorquez, M. A .Enrique, J. M.,& Andújar, J. M., (2010). A reliable, fast and low cost maximum power point tracker for photovoltaic applications. Solar energy, 84(1), 79-89.

Chapman, P. L. & Esram, T. (2007). Comparison of photovoltaic array maximum power point tracking techniques. IEEE Transactions on energy conversion, *22*(2), 439-449.

Christopher I. W, Ramesh R.(2013). Comparative study of P&O and InC MPPT algorithms. American Journal of Engineering Research (AJE),Vol. 2, no. 12, pp. 402-408.

Chun-hua, L., Xu, J., & Xin-jian, Z. (2009). Study on control strategy for photovoltaic energy systems based on recurrent fuzzy neural networks. In *2009 Fifth International Conference on Natural Computation* (Vol. 2, pp. 282-286). IEEE.

Dinçer, F. (2011). The analysis on photovoltaic electricity generation status, potential and policies of the leading countries in solar energy. Renewable and sustainable energy reviews, *15*(1), 713-720.

Dzung, P. Q., Lee, H. H., & Vu, N. T. D. (2010). The new MPPT algorithm using ANN-based PV. In *International Forum on Strategic Technology 2010* (pp. 402-407). IEEE.

El-khattam, W. Mohamed, A. E., & Marei, M. I. (2018). A maximum power point tracking technique for PV under partial shading condition. In 2018 8th IEEE India International Conference on Power Electronics *(IICPE)* (pp. 1-6). IEEE.

Farhat, S., Alaoui, R., Kahaji, A., & Bouhouch, L. (2013). Estimating the photovoltaic MPPT by artificial neural network. In 2013 International Renewable and Sustainable Energy Conference (IRSEC) (pp. 49-53). IEEE.

Fathi, M., & Parian, J. A. (2021). Intelligent MPPT for photovoltaic panels using a novel fuzzy logic and artificial neural networks based on evolutionary algorithms. Energy Reports, 7, 1338-1348.

Fujita, R. M.& Pelc, R. (2002). Renewable energy from the ocean. Marine Policy, 26(6), 471-479.

Gothandaraman, V., Ramaprabha, R., Kanimozhi, K., Mathur, B. L& Divya, R., (2011). Maximum power point tracking using GA-optimized artificial neural network for solar PV system. In 2011 1st International Conference on Electrical Energy Systems (pp. 264-268). IEEE.

Guerrero, J. M Mei, Q., &Shan, M., Liu, L. (2011). A novel improved variable step-size incremental-resistance MPPT method for PV systems. IEEE transactions on industrial electronics, 58(6), 2427-2434.

Gündoğdu, A & Çelikel, R. (2020). ANN-based MPPT algorithm for photovoltaic systems. Turkish Journal of Science and Technology, 15(2), 101-110.

Hagan, M. T. Demuth, H. B., De Jess, O., & Beale, M. H (2014). Neural network design. Martin Hagan.

Hoffmann, V. U. & Goetzberger, A. (2005). Photovoltaic solar energy generation. Springer Science & Business Media. (Vol. 112).

Huang, X & Huang, K., Li, W., (2011). MPPT of solar energy generating system with fuzzy control and artificial neural network. In 2011 International Conference of Information Technology, Computer Engineering and Management Sciences. Vol. 1, pp. 230-233. IEEE.

Ibrahim Henk, M Mahamudul, H.,& Saad, M. (2013). Photovoltaic system modeling with fuzzy logic based maximum power point tracking algorithm. International Journal of Photoenergy, 2013.

Jamasb, S .Moradi, M. H &. Reisi, A. R. (2013). Classification and comparison of maximum power point tracking techniques for photovoltaic system: A review. Renewable and sustainable energy reviews, 19, 433-443.

Jiang, M., Ghahremani, M., Dadfar, S., Chi, H., Abdallah, Y. N., & Furukawa, N. (2021). A novel combinatorial hybrid SFL–PS algorithm based neural network with perturb and observe for the MPPT controller of a hybrid PV-storage system. *Control Engineering Practice*, *114*, 104880.

Karami, N., Moubayed, N., & Outbib, R. (2017). General review and classification of different MPPT Techniques. *Renewable and Sustainable Energy Reviews*, *68*, 1-18.

Kassmi, K., Melhaoui, M., Lamkaddem, A., Deblecker, O. & Hirech, K., (2019). Multilevel DC/DC converter architectures for high performance PV system. Journal of Electrical Systems, 15(2).

Kayisli, Korhan. (2023) .Super Twisting Sliding Mode-Type 2 Fuzzy MPPT Control of Solar PV System with Parameter Optimization under Variable Irradiance Conditions. Ain Shams Engineering Journal, vol. 14, no. 1, 2023, p. 101950.

Ko, J. S., Huh, J. H., & Kim, J. C. (2020). Overview of maximum power point tracking methods for PV system in micro grid. *Electronics*, *9*(5), 816.

Kumaresh V, Malhotra, M., N, R., and Saravanaprabu.R., (2014). Literature Review on Solar MPPT Systems. Advance in Electronic and Electric Engineering, 4(3): 285-296.

Lazaro, A Salas, V., Olias, E., & Barrado, A. (2006). Review of the maximum power point tracking algorithms for stand-alone photovoltaic systems. Solar energy materials and solar cells, 90(11), 1555-1578.

Leow, W. Z., Irwanto, M., Ismail, B., Baharudin, N. H., Juliangga, R., Alam, H., & Masri, M. (2020). Photovoltaic powered DC-DC boost converter based on PID controller for battery charging system. In Journal of Physics: Conference Series. Vol. 1432, No. 1, p. 012055. IOP Publishing.

Litrán, S. P.,Vázquez, J. Orozco, M. I. A., R., Alcántara, F. J. & Salmerón, P (2009). Maximum Power Point Tracker of a photovoltaic system using sliding mode control. In *International Conference on Renewable Energies and Power Quality*.

Luo, L., Abdulkareem, S. S., Rezvani, A., Miveh, M. R., Samad, S., Aljojo, N., & Pazhoohesh, M. (2020). Optimal scheduling of a renewable based microgrid considering photovoltaic system and battery energy storage under uncertainty. *Journal of Energy Storage*, *28*, 101306.

M. A. SASI, (2017). Fuzzy logic control of MPPT controller for PV systems (Doctoral dissertation, Memorial University of Newfoundland.

Martins, D. C &Coelho, R. F. (2012). An optimized maximum power point tracking method based on pv surface temperature measurement. Sustainable Energy-Recent Studies, 89-114.

Massoud, A. M., Enjeti, P. N., Abdelsalam, A. K. & Ahmed, S., (2011). High-performance adaptive perturb and observe MPPT technique for photovoltaic-based microgrids. IEEE Transactions on power electronics, 26(4), 1010-1021.

Mathew, M. A. &Vinay, P., (2014). Modelling and Evaluation of MPPT Techniques based on a Ćuk Converter. International Journal of Engineering Research & Technology (IJERT), 3(5).

Matwoks, Matlab Help Center, https://www.mathworks.com/help/sps/ug/detailed-model-of-a-100-kw-grid-connected-pv-array.html. Last access date 20.05.2023.

Mekhilef, S. & Safari, A. (2010). Simulation and hardware implementation of incremental conductance MPPT with direct control method using cuk converter. IEEE transactions on industrial electronics, 58(4), 1154-1161.

Meng, X., Gao, F., & Xu, T. (2020). Optimized Design of Artificial Neural Network based Global MPPT for PV System under Partial Shading Conditions. In *2020 IEEE 9th International Power Electronics and Motion Control Conference (IPEMC2020-ECCE Asia)* (pp. 1729-1733). IEEE.

Meng, X., Gao, F., Xu, T., & Zhang, C. (2021). Fast Two-Stage Global Maximum Power Point Tracking for Grid-Tied String PV Inverter Using Characteristics Mapping Principle. *IEEE Journal of Emerging and Selected Topics in Power Electronics*, *10*(1), 564-574.

Bennett, T., Messenger, R & Zilouchian, A. (2013). A proposed maximum power point tracking algorithm based on a new testing standard. Solar Energy, *89*, 23-41.

Mohamed, M. S., Abdellatif, W. S., Barakat, S., & Brisha, A. (2021). A Fuzzy Logic Controller Based MPPT Technique for Photovoltaic Generation System. International Journal on Electrical Engineering & Informatics, 13(2).

Nasser, K. W., Yaqoob, S. J., & Hassoun, Z. A. (2021). Improved dynamic performance of photovoltaic panel using fuzzy logic-MPPT algorithm. Indonesian Journal of Electrical Engineering and Computer Science, 21(2), 617-624.

Mohan, N. and Undeland, T.M. (2007) Power Electronics: Converters, Applications, and Design. John Wiley & Sons, Hoboken.

Onar, O. C.& Khaligh, A. (2017). Energy harvesting: solar, wind, and ocean energy conversion systems. CRC press.

Osakada, M, Hoshino, T Hussein, K. H., & Muta, I., (1995). Maximum photovoltaic power tracking: an algorithm for rapidly changing atmospheric conditions. IEE Proceedings-Generation, Transmission and Distribution, 142(1), 59-64.

Ouali, M & Salah, C. B. (2011). Comparison of fuzzy logic and neural network in maximum power point tracker for PV systems. Electric Power Systems Research, 81(1), 43-50.

Patel, M. R. (2006). Design, analysis, and operation wind and solar power systems. International Standard Book Number-10: 0-8493-1570-0.

Pikutis, M Martavicius, R., & Vasarevicius, D. (2012). Application of artificial neural networks for maximum power point tracking of photovoltaic panels. Elektronika ir elektrotechnika, 18(10), 65-68

Powers, M. J. &Sullivan, C. R. (1993). A high-efficiency maximum power point tracker for photovoltaic arrays in a solar-powered race vehicle. In Proceedings of IEEE Power Electronics Specialist Conference-PESC'93 (pp. 574-580). IEEE.

Pradhan, R. & Subudhi, B. (2012). A comparative study on maximum power point tracking techniques for photovoltaic power systems. IEEE transactions on Sustainable Energy, 4(1), 89-98.

Rahman, M. d. Motakabbir, and M. S. Islam. (2019). Artificial Neural Network Based Maximum Power Point Tracking of a Photovoltaic System. 2019 3rd International Conference on Electrical, Computer & Telecommunication Engineering (ICECTE).

Rajesh, R., & Mabel, M. C. (2015). A comprehensive review of photovoltaic systems. Renewable and sustainable energy reviews, *51*, 231-248.

Rodriguez-Resendiz, Villegas-Mier, C. G., J., Álvarez-Alvarado, J. M., Rodriguez-Resendiz, H., Herrera-Navarro, A. M., & Rodríguez-Abreo, O. (2021). Artificial neural networks in MPPT algorithms for optimization of photovoltaic power systems: A review. Micromachines, *12*(10), 1260.

Roy, R. B., Rokonuzzaman, M., Amin, N., Mishu, M. K., Alahakoon, S., Rahman, S., ... & Pasupuleti, J. (2021). A Comparative Performance Analysis of ANN Algorithms for MPPT Energy Harvesting in Solar PV System. IEEE Access, vol. 9, pp. 102137–102152.

Saravana, P. R. Kumaresh, V., & Malhotra, M., (2014). Literature review on solar MPPT systems. Advance in Electronic and Electric Engineering, 4(3), 285-296.

Shahid, M., & Singh, H. (2016). Soft Computing Techniques FUZZY and ANN based MPPT for Grid Tied PV. *International Journal of Engineering Research*, *5*(05).

Shih, T. L. & Lu, H. C. (2010). Design of DC/DC Boost converter with FNN solar cell Maximum Power Point Tracking controller. In 2010 5th IEEE Conference on Industrial Electronics and Applications (pp. 802-807). IEEE.

Shujaee, K. Boico, F.,& Lehman, B. (2007). Solar battery chargers for NiMH batteries. IEEE Transactions on Power Electronics, 22(5), 1600-1609.

Silvestre, S., Chouder, A., & Rahmani, L., & Sadaoui, N. (2012). Modeling and simulation of a grid connected PV system based on the evaluation of main PV module parameters. Simulation Modelling Practice and Theory, 20(1), 46-58.

Souba, J. R. Moumouni, Y., & Baker, R. J. (2016). Analysis of a residential 5kW grid-tied photovoltaic system. In 2016 Clemson university power systems conference (PSC) (pp. 1-4). IEEE.

Veerachary, M. (2008, December). Maximum Power point tracking algorithm for non-linear DC Sources. In *2008 IEEE Region 10 and the Third international Conference on Industrial and Information Systems* (pp. 1-6). IEEE.

Vitelli, M Femia, N., Petrone, G., &Spagnuolo, G. (2004). Optimizing sampling rate of P&O MPPT technique. In 2004 IEEE 35th Annual Power Electronics Specialists Conference (IEEE Cat. No. 04CH37551.Vol. 3, pp. 1945-1949). IEEE.

Yüksek, G., & Mete, A. N. (2023). A P&O Based Variable Step Size MPPT Algorithm for Photovoltaic Applications. *Gazi University Journal of Science*, *36*(2), 608-622.

Zaki, A. M., Amer, S. I., & Mostafa, M. (2012). Maximum power point tracking for PV system using advanced neural networks technique. International Journal of Emerging Technology and Advanced Engineering, 2(12), 58-63.

Zhao, Z & Eltawil, M. A. (2013). MPPT techniques for photovoltaic applicatio*ns.* Renewable and sustainable energy reviews, 25, 793-813.

7. ÖZGEÇMİŞ